

Machine Learning-Based Prediction on Normalized Cumulative Dissipated Energy (NCDE) of Reinforced Concrete Shear Walls

Negar Dokhtmirzahasanvahid

Contents

1	Introduction	3
2	Dataset and Feature Exploration	4
2.1	Dataset Overview	4
2.2	Missing Values	4
2.3	Normalization Strategy	4
2.4	Target Variable: NCDE Distribution	4
2.5	Feature Transformations	5
2.6	Feature Dictionary	8
3	Feature Distributions: Visual Exploration	8
3.1	Summary	15
4	NAM Configuration and Model Tuning	15
4.1	Hyperparameter Optimization	15
4.1.1	Hidden Layer Architecture	15
4.1.2	Batch Size Effects	16
4.2	Model Performance	16
4.2.1	Final Configuration	16
5	NAM Feature Learning and Interpretation	17
5.1	Feature Function Analysis	17
5.1.1	Primary Feature Effects	17
5.2	Training Dynamics	18
5.3	Feature-NCDE Relationships	19
5.4	Feature Importance Analysis	19
5.4.1	Top Contributing Features	19
5.4.2	Deep Feature Analysis	20

6 Baseline Model Comparison	21
6.1 Random Forest Analysis	21
6.1.1 Performance Metrics	21
6.2 XGBoost Analysis	22
6.2.1 Performance Metrics	22
6.3 Comparative Analysis	22
6.3.1 Quantitative Comparison	22
7 Model Comparison and Residual Analysis	23
7.1 Prediction Performance	23
7.1.1 R-squared Analysis	23
7.2 Residual Analysis	23
7.2.1 Distribution Characteristics	23
7.2.2 Normality Assessment	24
7.3 Statistical Significance	24
7.3.1 ANOVA Results	24
7.4 Statistical Comparison: ANOVA and Tukey's HSD	26
8 SHAP-Based Interpretability Analysis	27
8.1 Global SHAP Importance (Random Forest)	27
8.2 SHAP Summary Plot	28
8.3 Dependence Plots for Interactions	28
8.4 Interpretation Summary	29
9 XGBoost SHAP Analysis	30
9.1 Global Feature Importance	30
9.2 SHAP Dependence Analysis	31
9.3 SHAP Value Distribution	32
9.4 Summary	32
10 Model Comparison	33
10.1 Directional Agreement	33
10.2 Directional Disagreement	34
10.3 Feature Effect Comparison	35
10.3.1 Boundary Width (b_0)	35
10.3.2 Wall Height (hw)	35
10.3.3 Wall Length (lw)	36
10.3.4 Moment–Shear Ratio ($M/(V lw)$)	36
10.3.5 Shear Reinforcement Ratio (ρ_{sh})	36
10.4 Feature Importance Comparison	37
11 Conclusion	37
11.1 Key Takeaways	37
11.2 Detailed Analysis	38

1 Introduction

Seismic performance of reinforced concrete shear walls is governed by a combination of geometric dimensions, material properties, and reinforcement detailing. In particular, the *Normalized Cumulative Dissipated Energy* (NCDE) is a key metric for quantifying how much cyclic energy a wall can absorb before failure. Accurately predicting NCDE enables engineers to design more resilient structures under earthquake loading.

This study implements and compares three distinct machine-learning approaches:

- **Neural Additive Model (NAM):** A smooth, interpretable model that learns a separate nonparametric function $g_j(x_j)$ for each feature x_j , so that

$$\hat{y} = \beta_0 + \sum_j g_j(x_j).$$

Each feature-specific function g_j is estimated using a neural network with B-spline basis expansions (10 knots per feature) and ReLU activation functions, allowing for flexible non-linear relationships while maintaining interpretability. NAM provides clear visualizations of each feature's continuous contribution.

- **Random Forest (RF):** An ensemble of decision trees that captures complex interactions and nonlinearities. Feature contributions are explained via SHAP values, which quantify each variable's marginal impact on the RF prediction.
- **XGBoost (XGB):** A gradient-boosted tree method optimized for predictive accuracy. We again employ SHAP to interpret feature effects, acknowledging that boosted trees can amplify or invert relationships seen in RF or NAM.

We standardize and preprocess a database of 312 specimens, each described by 18 geometric and reinforcement features (e.g. wall length lw , thickness tw , transverse yield strength f_{ysh} , shear ratio ρ_{sh}). Models are evaluated on hold-out sets using R^2 , RMSE, MAE, and explained variance.

The following sections present:

1. *Global performance metrics* (Section 6), comparing overall predictive accuracy.
2. *Directional agreement and disagreement* (Tables 6 and 7), identifying which features exhibit consistent or conflicting effect signs across models.
3. *Feature effect comparisons* (Figures 36 through 40), contrasting NAM's smooth functions with RF/XGB SHAP scatterplots on key variables.
4. *Feature importance analysis* (Figure 41), showing relative weighting of inputs in each model.
5. *Conclusion* (Section 11), synthesizing insights and recommending best practices for seismic-design integration.

By triangulating these three modeling paradigms, we aim to balance predictive performance with mechanistic transparency, offering practical guidance for both researchers and structural engineers.

2 Dataset and Feature Exploration

2.1 Dataset Overview

The original dataset contains 312 reinforced concrete shear wall specimens. Each entry describes 25 features relating to material properties, geometric configurations, reinforcement details, and load conditions. The target variable, NCDE (Normalized Cumulative Dissipated Energy), quantifies the seismic energy absorption capacity of each wall.

2.2 Missing Values

Several key features have missing values:

- **fysh** (Transverse boundary reinforcement yield strength): 32.1%
- **fybl** (Vertical boundary reinforcement yield strength): 9.3%
- **ρ_{sh}** (Transverse boundary reinforcement ratio): 30.8%
- **ρ_{bl}** (Vertical boundary reinforcement ratio): 10.3%

Missing values were handled via rank-based imputation after transformation for heavily skewed distributions.

2.3 Normalization Strategy

To ensure numerical stability and uniform treatment across models:

- A **MinMaxScaler** was applied to all input features and the target variable.
- Scaling was performed using `feature_range=(-1, 1)`.
- Final dataset splits:
 - **Training set (X_{train})**: 249 samples
 - **Testing set (X_{test})**: 63 samples
 - **Target vectors**: y_{train}, y_{test} matching the same indices

2.4 Target Variable: NCDE Distribution

The output variable NCDE, even after normalization, exhibits strong left-skewed behavior. Most samples have low energy dissipation values, with very few high-energy outliers. This has implications for model bias and sensitivity to rare high-performing wall configurations.

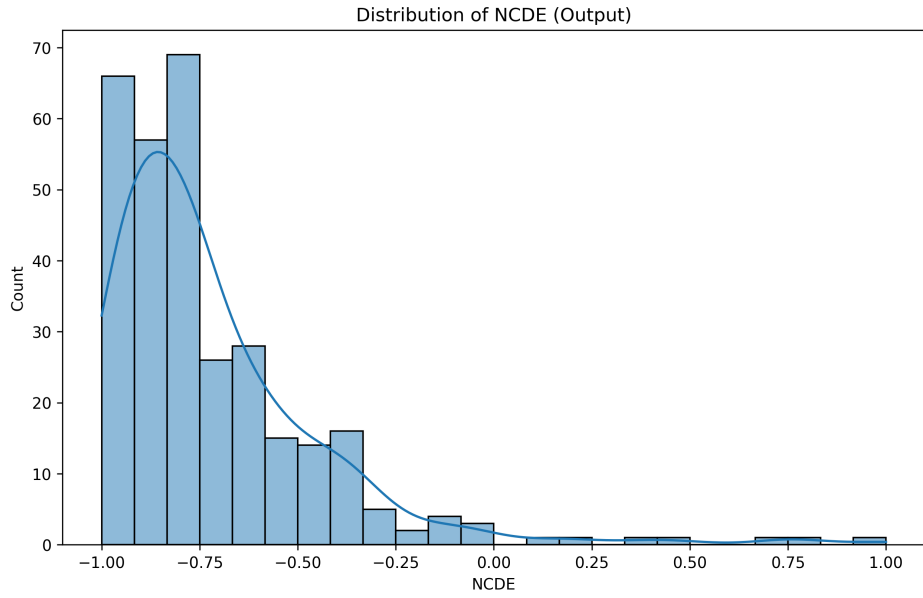


Figure 1: Distribution of **NCDE** (Normalized cumulative dissipated energy). Output variable is highly left-skewed, with the majority of samples concentrated in the $[-1, -0.5]$ range. Indicates most walls dissipate low energy under seismic loading.

2.5 Feature Transformations

Example 1: fysh (Transverse boundary reinforcement yield strength)

Initial skewness: 2.17. Applied transforms:

- **Log1p**: skew = -1.37
- **Power**: skew = -0.41
- **Rank**: skew = 0.00

Rank transform selected.

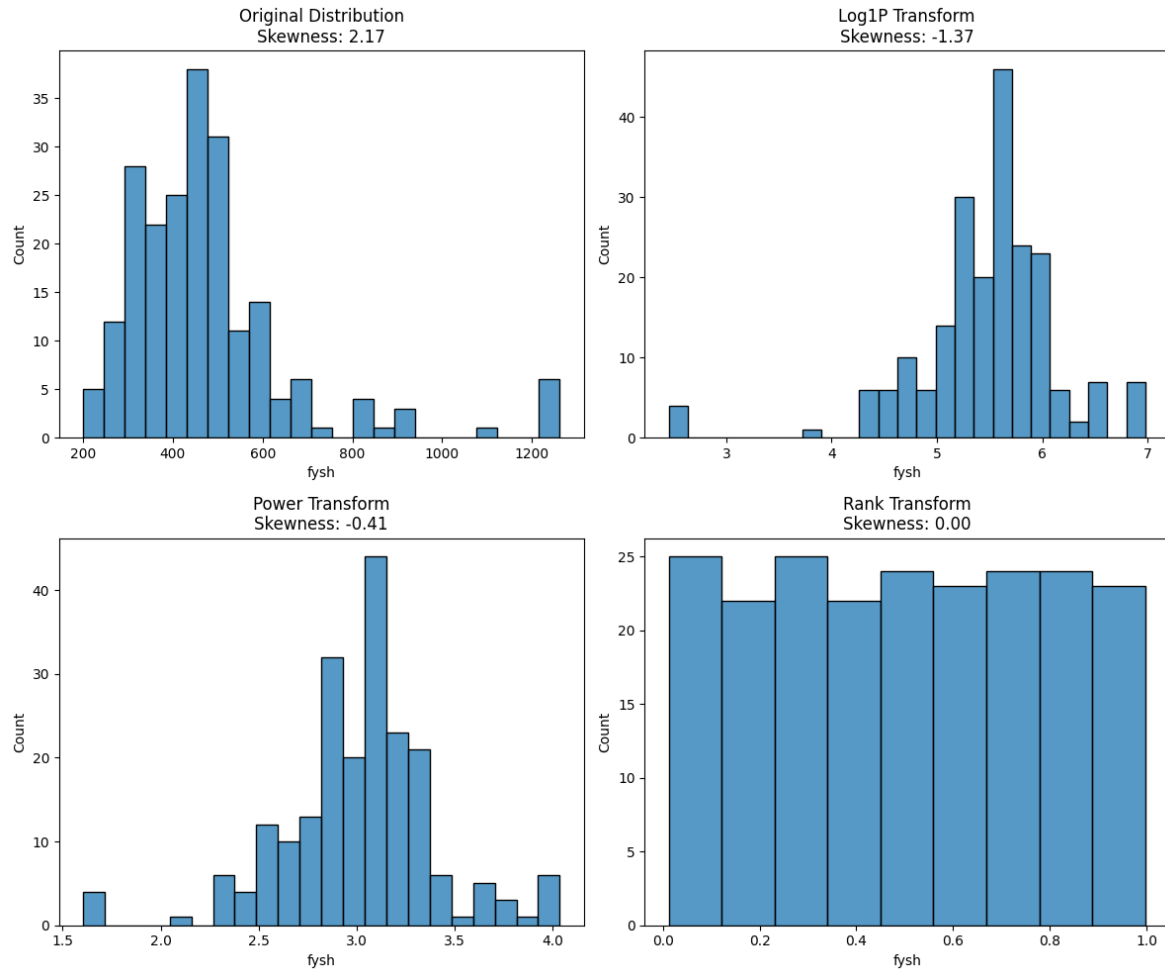


Figure 2: Distribution of **fysh** before and after transformation.

Example 2: ρ_{sh} (Transverse boundary reinforcement ratio)

Initial skewness: 5.07, kurtosis: 40.30. Transformation outcomes:

- **Log1p:** skew = 4.87
- **Power:** skew = 0.43
- **Rank:** skew = 0.00

Rank transform used for model input.

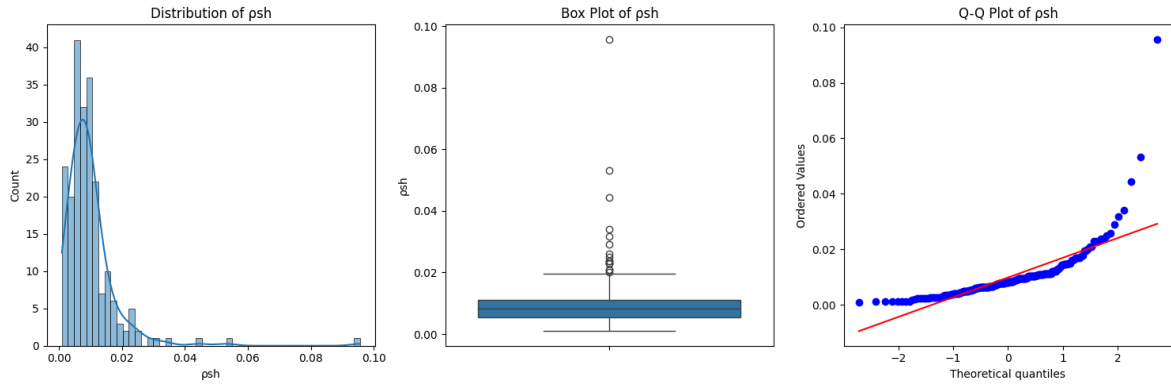


Figure 3: Distribution, boxplot, and Q-Q plot for ρsh .

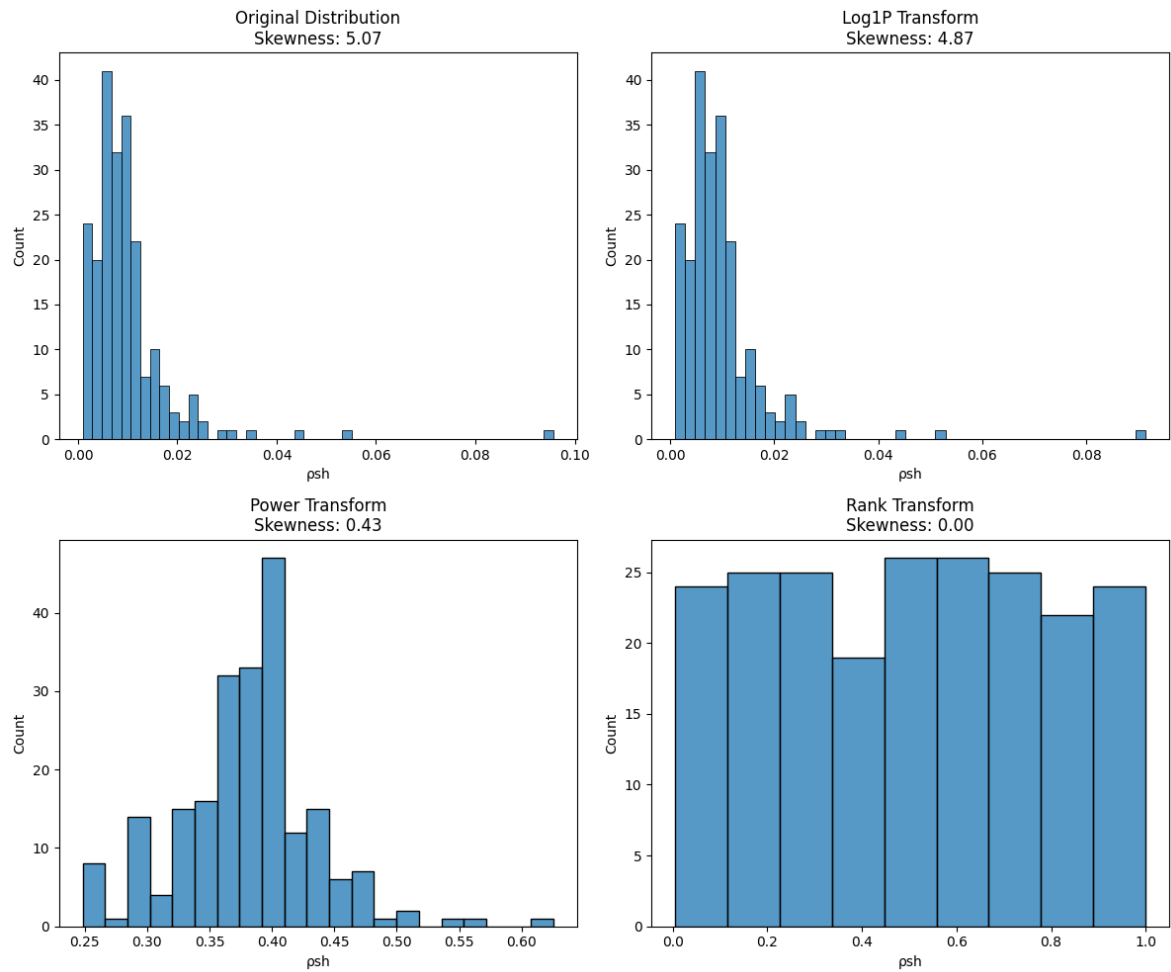


Figure 4: Distribution of ρsh before and after transformation.

2.6 Feature Dictionary

Below is a subset (10 out of 18) of the most influential features used in our analysis. The complete feature set is available in the supplementary materials.

- lw , hw , tw : Wall geometry (length, height, thickness)
- $f'c$: Concrete compressive strength
- $fysh$, $fybl$: Reinforcement yield strengths
- ρsh , ρbl : Reinforcement ratios
- $P/(Agf'c)$: Axial load ratio
- AR : Aspect ratio
- M/Vlw : Flexure-to-shear ratio

3 Feature Distributions: Visual Exploration

To better understand the statistical behavior of key features, we visualized their distributions after normalization. Several features remain skewed despite normalization, which can influence model training dynamics.

1. Boundary Element Geometry

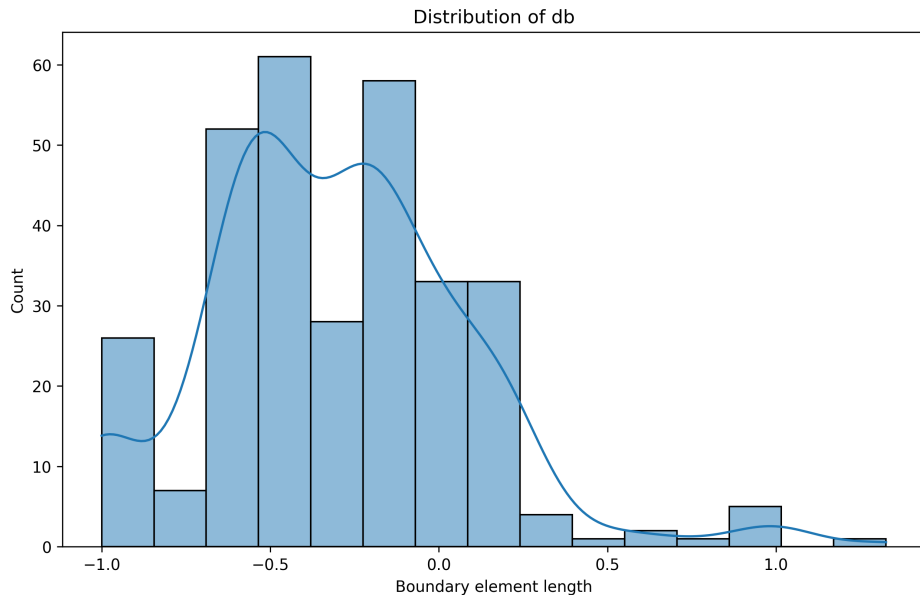


Figure 5: Distribution of db (Boundary element length). The distribution is roughly bell-shaped with a slight left skew. Most walls have moderately sized boundary lengths.

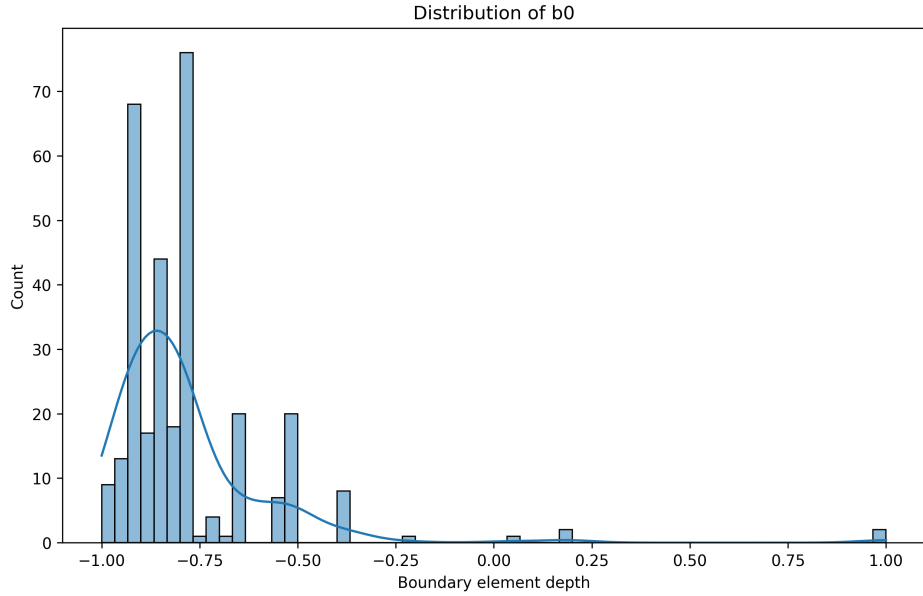


Figure 6: Distribution of \mathbf{b}_0 (Boundary element depth). The distribution is highly left-skewed, with a majority of values clustered near the lower boundary.

4. Feature Boxplot Distribution

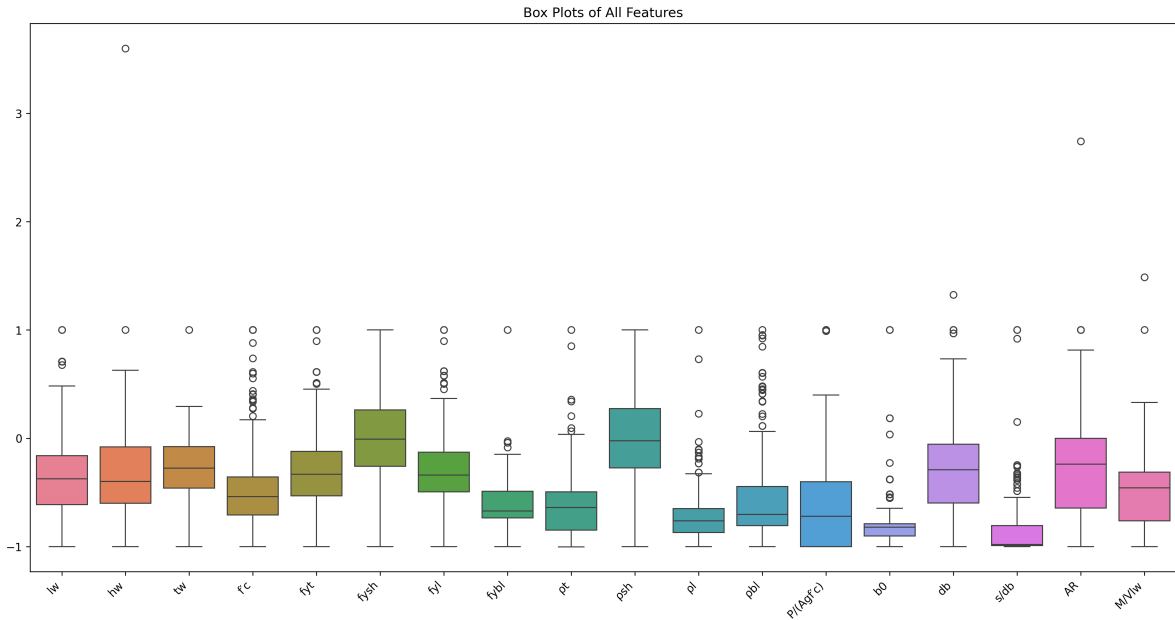


Figure 7: Box plots of all input features after normalization.

Observation: Several features like $fybl$, psh , and $P/(Agf'C)$ exhibit substantial outliers and skewness. These could influence gradient-based optimization or amplify variance in learning curves.

2. Structural Ratios and Proportions

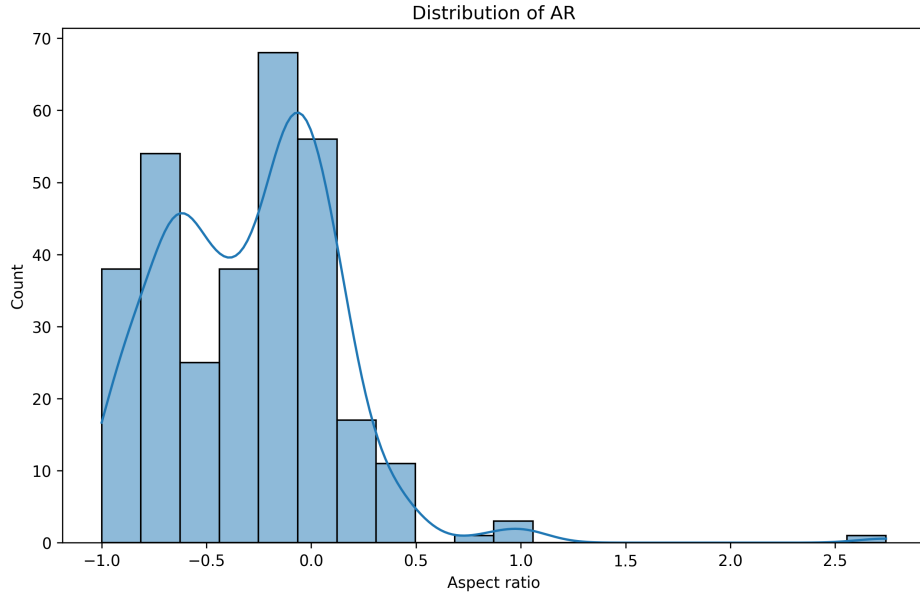


Figure 8: Distribution of AR (Aspect ratio). Most aspect ratios are low, indicating squat walls. A few samples with higher values represent slender geometries.

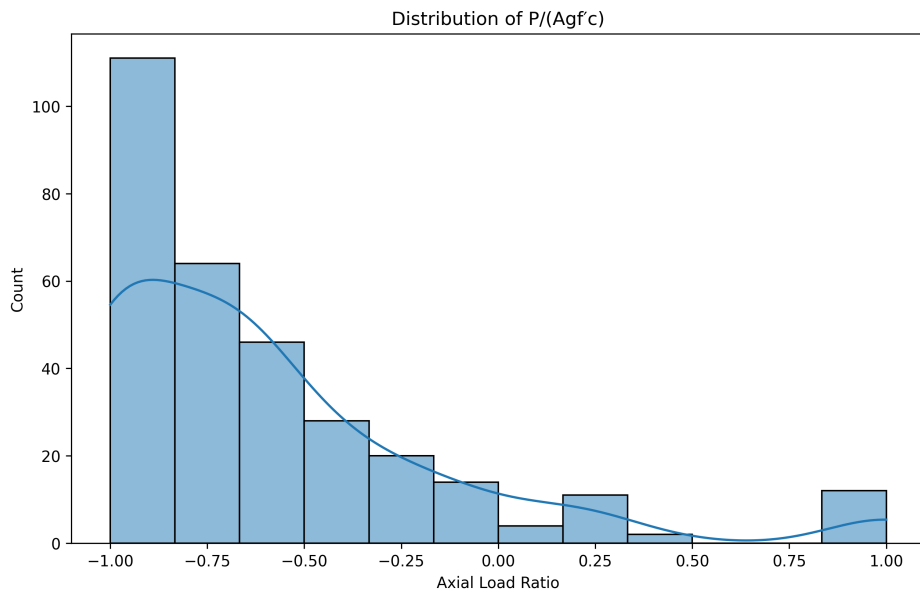


Figure 9: Distribution of $P/\text{Agf'c}$ (Axial Load Ratio). Strongly left-skewed, indicating that most walls carry relatively low axial stress relative to their concrete strength.

3. Material Properties

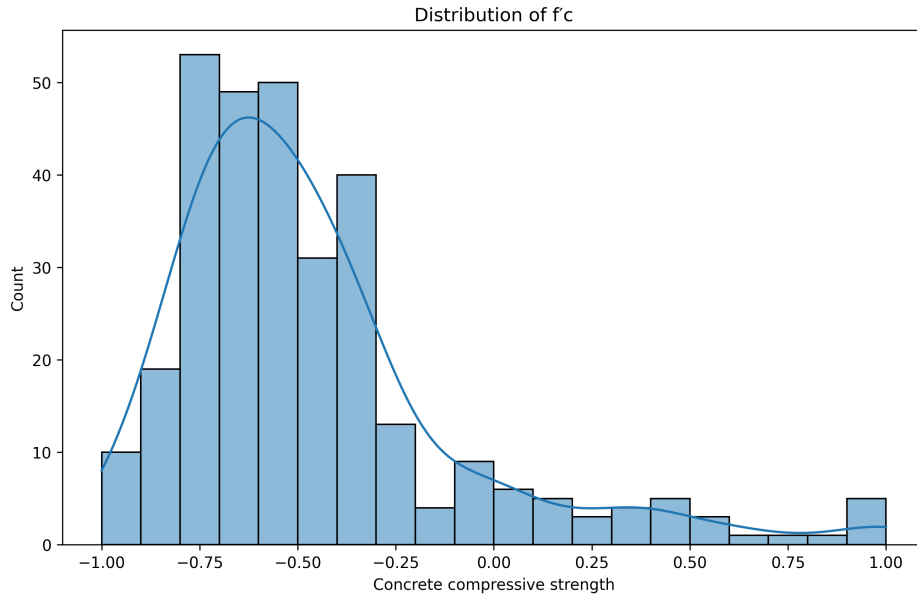


Figure 10: Distribution of $f'c$ (Concrete compressive strength). While normalized, this feature retains mild right skewness, suggesting a prevalence of lower-strength concrete.

4. Reinforcement Yield Strengths

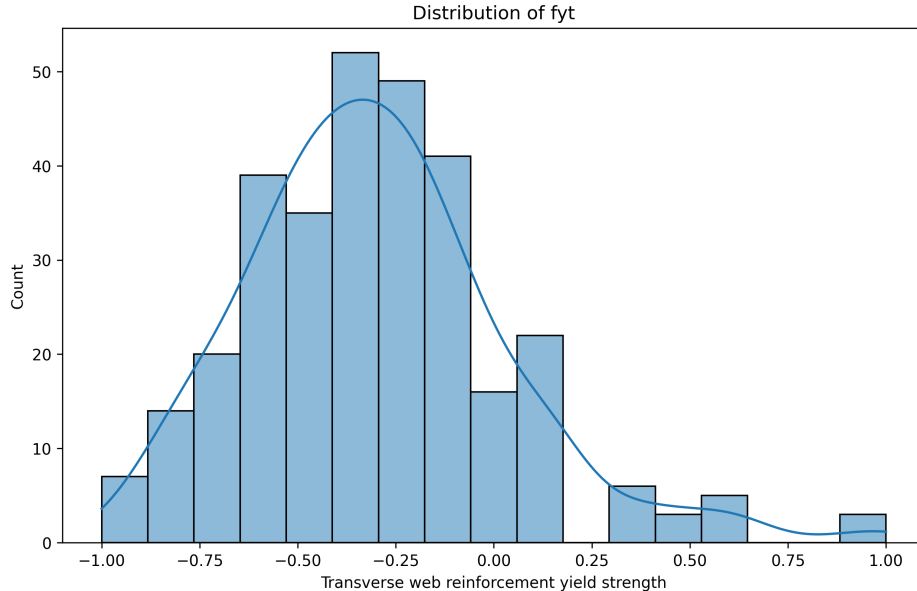


Figure 11: Distribution of fy_t (Transverse web reinforcement yield strength). Nearly symmetric with a peak slightly left of center.

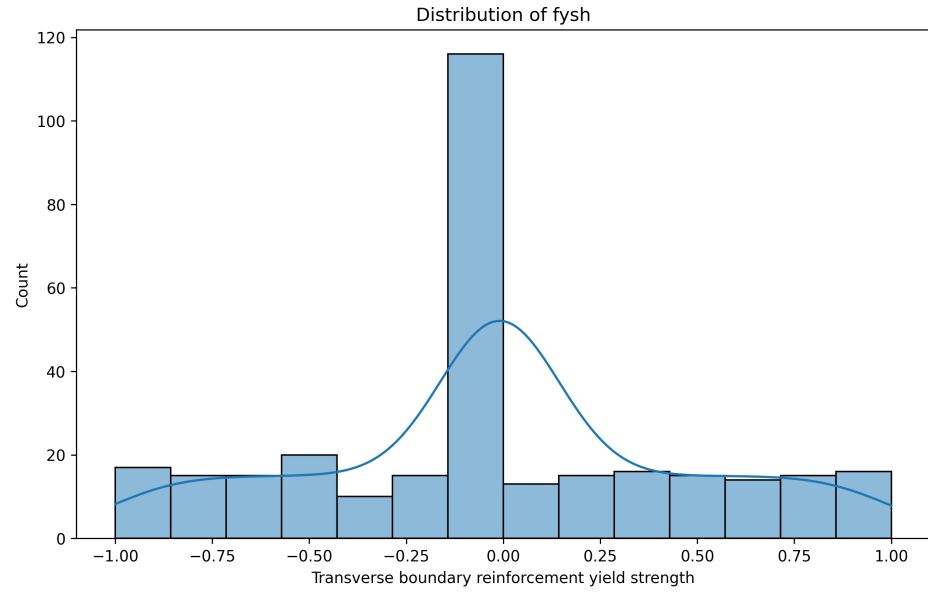


Figure 12: Distribution of **fysh** (Transverse boundary reinforcement yield strength). Rank transformation resulted in a centered and symmetric distribution.

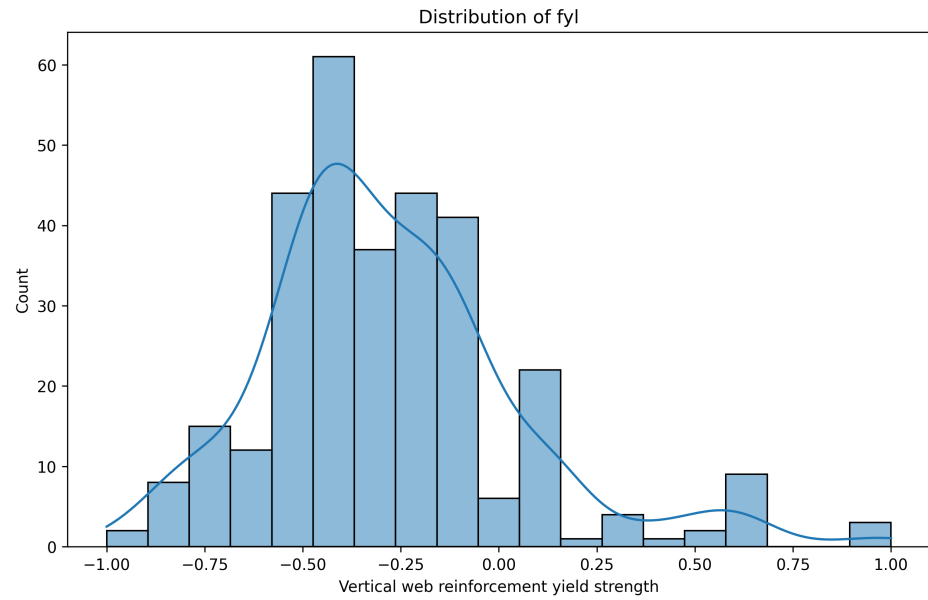


Figure 13: Distribution of **fyl** (Vertical web reinforcement yield strength). Displays mild skew with a broad middle concentration.

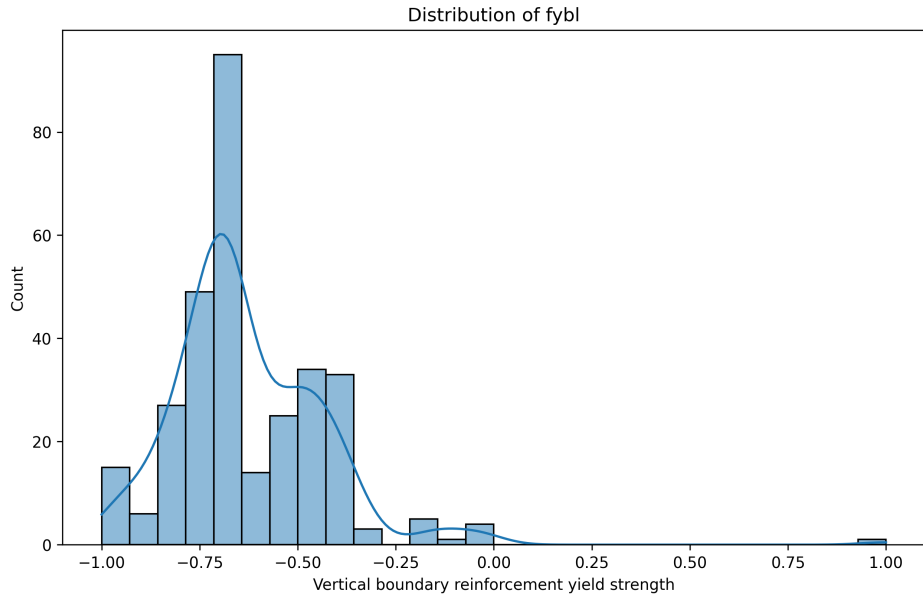


Figure 14: Distribution of **fybl** (Vertical boundary reinforcement yield strength). Strong left skew with outliers in the high-strength range.

5. Target Variable: NCDE

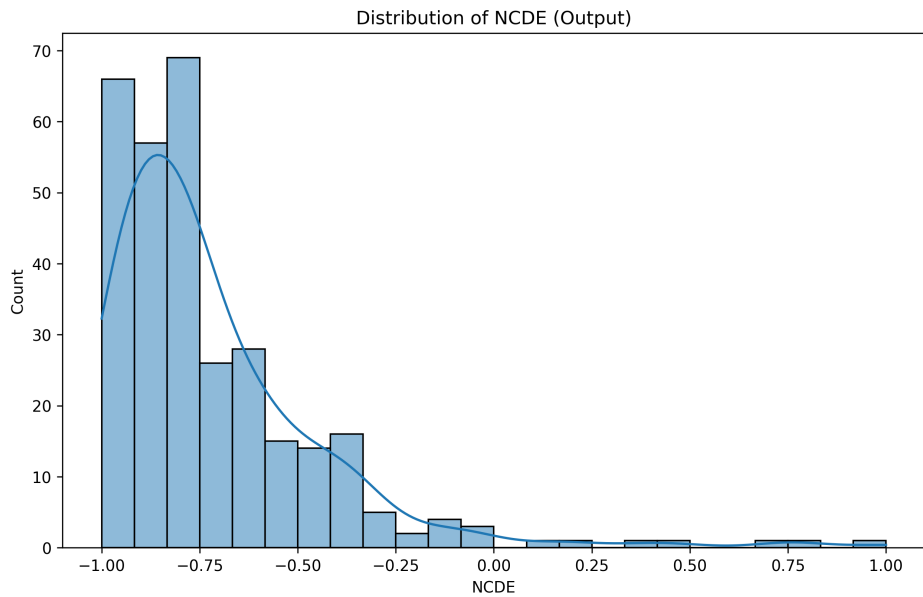


Figure 15: Distribution of **NCDE** (Normalized cumulative dissipated energy). Output variable is highly left-skewed, with the majority of samples concentrated in the $[-1, -0.5]$ range. Indicates most walls dissipate low energy under seismic loading.

6. Inter-feature Correlation Matrix

To assess multicollinearity and identify highly dependent features, we computed the Pearson correlation coefficients across all normalized input variables. The heatmap in Figure 16 visualizes pairwise relationships between features.

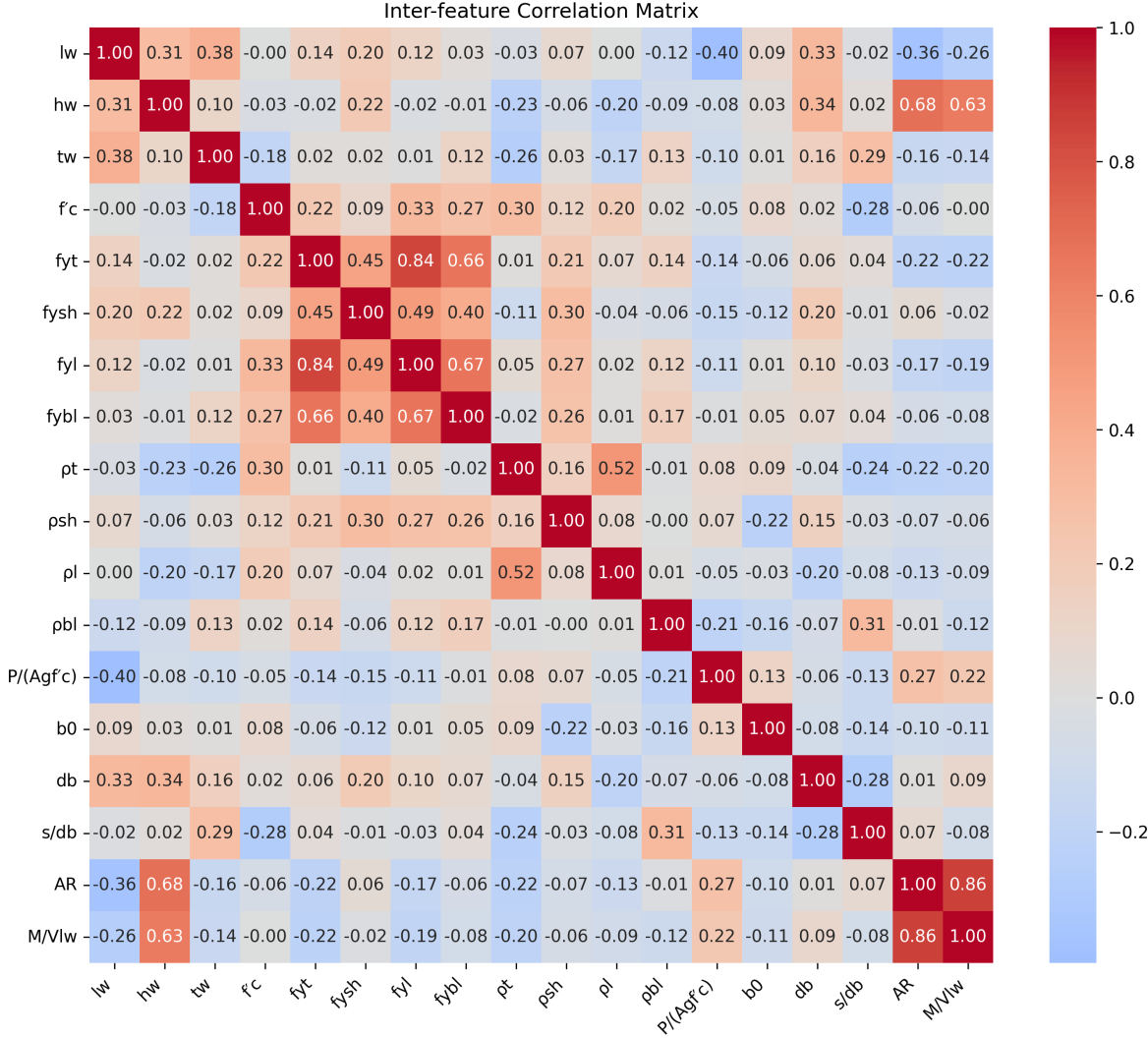


Figure 16: Correlation heatmap for normalized features. Warmer colors indicate positive correlations, cooler tones represent negative correlations.

Key observations:

- **fyt–fyl:** Strong positive correlation ($r = 0.84$), suggesting similar reinforcement properties for transverse and vertical web reinforcements.
- **fybl–fyt:** High correlation ($r = 0.66$), implying boundary and web reinforcement strengths tend to co-vary.

- **AR–hw**: Very strong correlation ($r = 0.68$), expected since aspect ratio depends on height.
- **AR–M/Vlw**: Extremely strong positive correlation ($r = 0.86$), indicating high multicollinearity. These two features may need to be treated with care to avoid redundancy.
- **P/(Agf'c)–lw**: Moderate negative correlation ($r = -0.40$), hinting that longer walls tend to carry lower normalized axial loads.

These correlations guided both the feature selection and the interpretability analysis, especially where models might conflate effects due to tightly coupled inputs.

3.1 Summary

The preprocessing pipeline involved missing value imputation, transformation of highly skewed features, and uniform normalization. Target distribution remains heavily skewed, making model interpretation and fairness essential. Rank-based transformations were especially effective for controlling outlier-heavy structural features.

4 NAM Configuration and Model Tuning

4.1 Hyperparameter Optimization

4.1.1 Hidden Layer Architecture

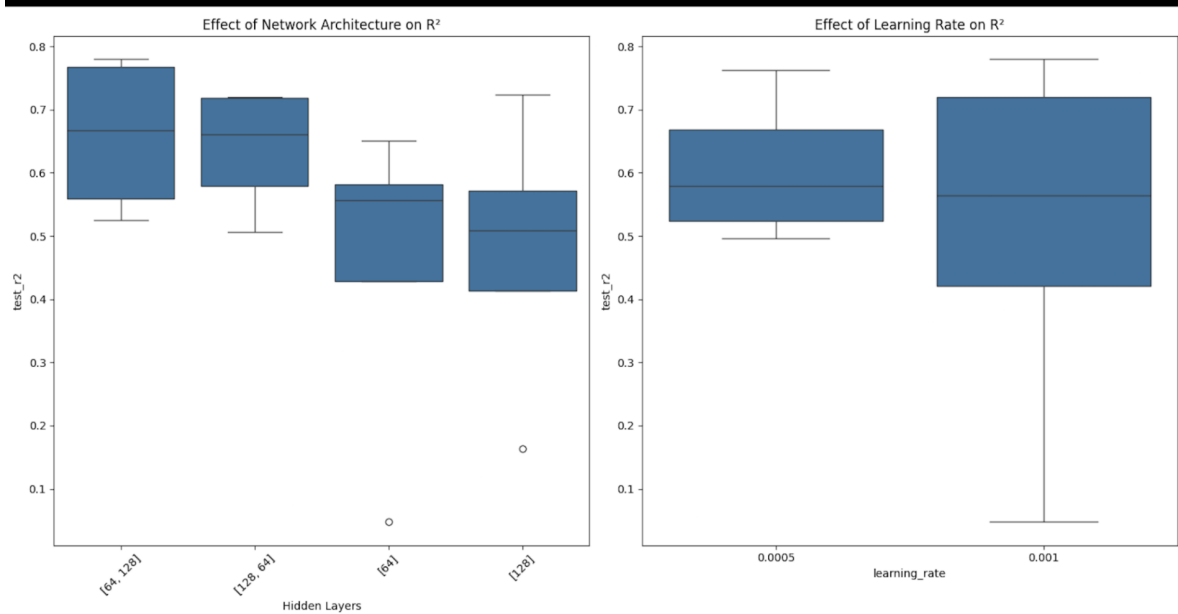


Figure 17: Effect of network architecture (left) and learning rate (right) on test R^2 .

Observation: Deeper architectures consistently outperformed shallower ones. The configuration [64, 128] produced the highest median test R^2 , indicating that multi-layer representations help NAMs learn non-linear interactions more effectively. The learning rate of 0.001 led to slightly higher variance in performance but produced higher upper bounds.

4.1.2 Batch Size Effects

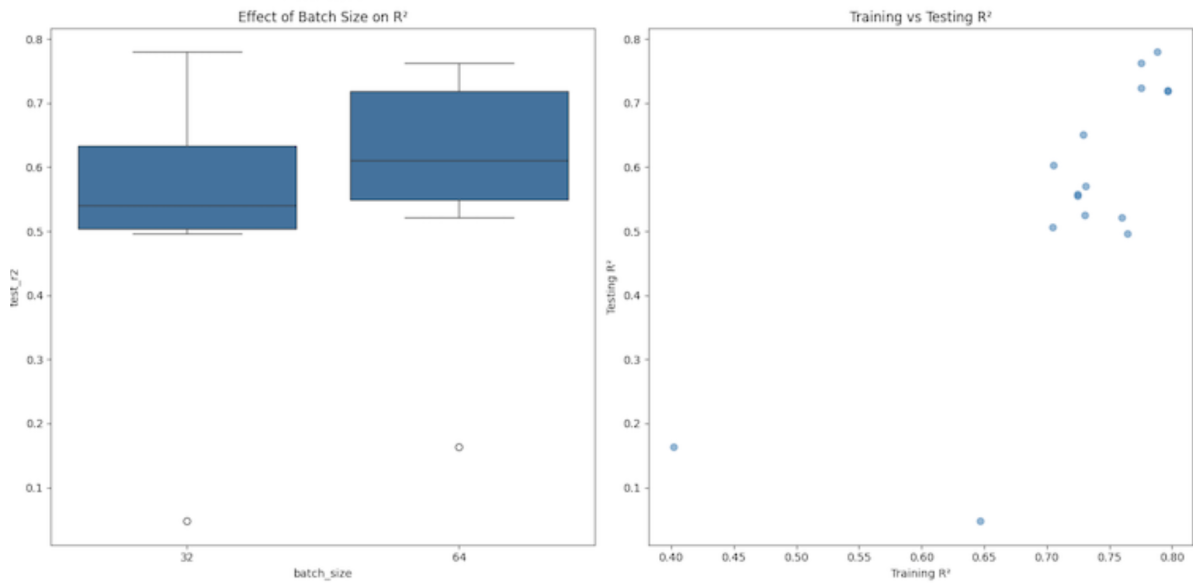


Figure 18: Effect of batch size on test R^2 (left) and generalization gap visualized via train vs test R^2 (right).

Observation: Larger batch size (64) resulted in higher median test R^2 compared to 32. However, it also introduced slightly more variance in performance across runs. The right plot confirms that models with higher training scores generally retained their advantage during testing, indicating low overfitting and good generalization.

4.2 Model Performance

4.2.1 Final Configuration

The final model was selected based on validation R^2 performance. Its configuration and evaluation metrics are as follows:

- **Hidden Layers:** [64, 128]
- **Learning Rate:** 0.001
- **Batch Size:** 32
- **Train RMSE / MAE / R^2 :** 177.5 / 114.3 / 0.788

- Test RMSE / MAE / R^2 : 218.0 / 147.7 / 0.7796
- Explained Variance (Train): 0.7881

Conclusion: This configuration balances expressive capacity and regularization. The close train-test performance metrics suggest the model is not overfitting and learns generalizable patterns in the structural data.

5 NAM Feature Learning and Interpretation

5.1 Feature Function Analysis

5.1.1 Primary Feature Effects

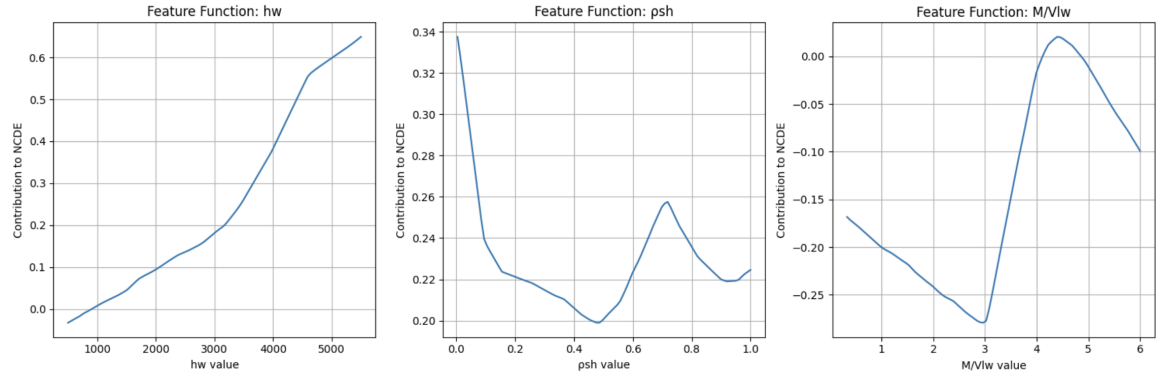


Figure 19: NAM-learned univariate functions for three impactful features: wall height (**hw**), transverse boundary reinforcement ratio (ρ_{sh}), and shear span ratio (**M/Vlw**).

Wall Height (hw)

- **Monotonic, linear, and positively sloped.**
- Contribution range: **0.6814**.
- Interpretation: Taller walls are more effective at dissipating seismic energy, likely due to better deformation capacity.

Transverse Boundary Reinforcement Ratio (ρ_{sh})

- **Non-monotonic, nonlinear.**
- Contribution range: **0.1385**.
- Interpretation: Small-to-moderate reinforcement may enhance energy dissipation, but excessive reinforcement could backfire, possibly due to brittle failure or ineffective detailing.

Shear Span Ratio (M/Vlw)

- Non-monotonic, nonlinear.
- Contribution range: **0.2998**.
- Interpretation: Moderate shear span ratios reduce NCDE. However, at extremes, structural detailing or dominant failure modes might paradoxically improve energy dissipation.

5.2 Training Dynamics

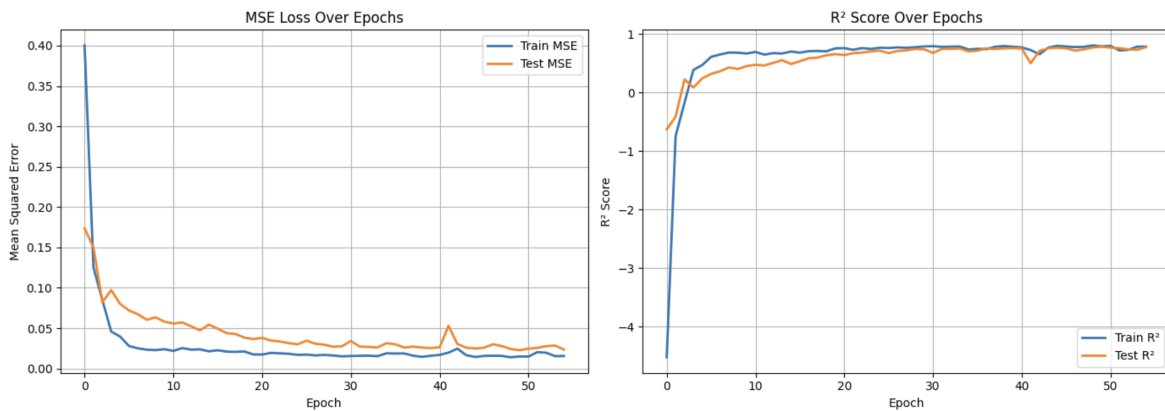


Figure 20: Left: MSE loss over 50 epochs. Right: R^2 score progression.

Observation: The model converges rapidly in the first 10 epochs. Both training and test R^2 stabilize around 0.78–0.79, with minimal overfitting. This suggests effective generalization across folds.

5.3 Feature-NCDE Relationships

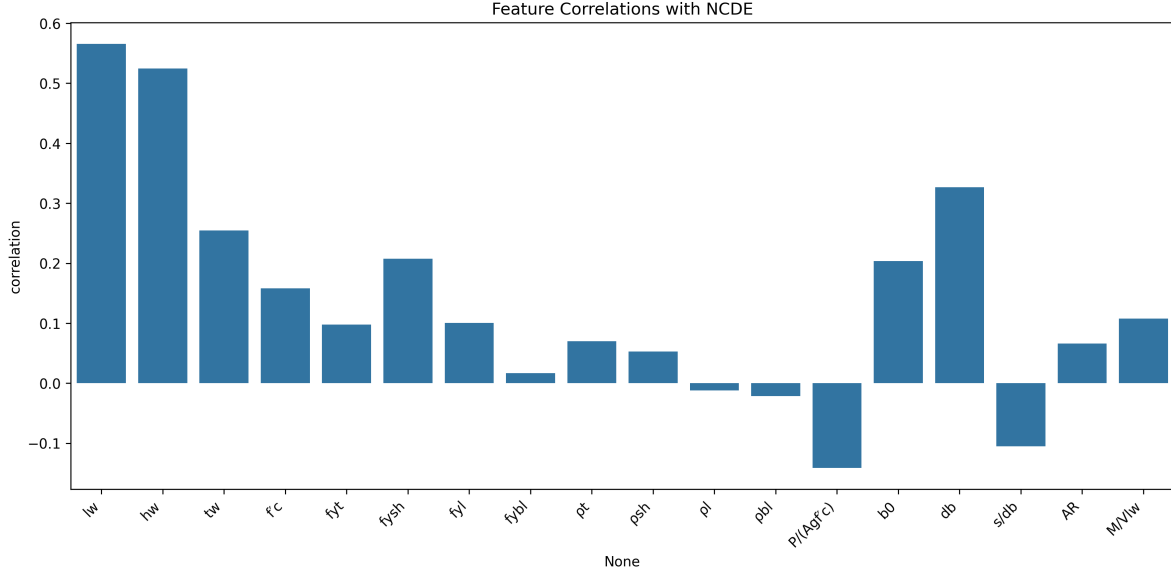


Figure 21: Pearson correlation of each feature with NCDE.

Observation: Features such as **lw**, **hw**, and **db** are strongly positively correlated with NCDE, while features like **P/(Agf'c)** and **s/db** exhibit negative correlations. However, correlation alone fails to capture nonlinearity, as clarified by NAM’s contribution functions.

5.4 Feature Importance Analysis

5.4.1 Top Contributing Features

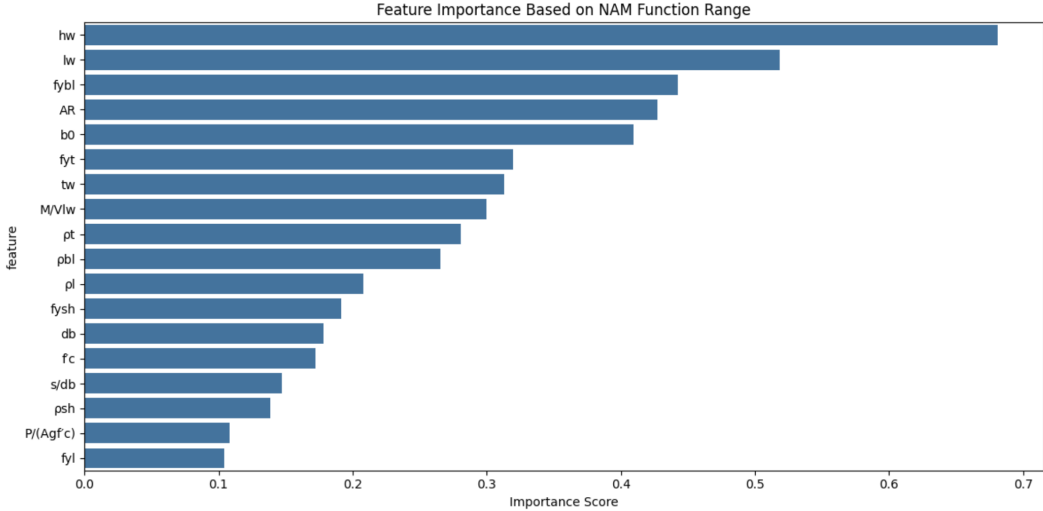


Figure 22: Feature importance ranked by NAM function contribution range.

Top features:

- **hw** (Wall Height)
- **lw** (Wall Length)
- **fybl** (Vertical Boundary Yield Strength)
- **AR** (Aspect Ratio)
- **b0** (Boundary Depth)

These top features are either directly geometric or boundary-related, reinforcing the conclusion that energy dissipation in shear walls is governed predominantly by physical form and reinforcement configuration.

5.4.2 Deep Feature Analysis

To gain actionable structural insight, we analyzed the feature importance values extracted from the final NAM model, using the range of each feature function as a proxy for its influence on NCDE. This section categorizes the features by relative impact and unpacks their structural implications.

1. Most Influential Features

Wall Height (hw) and **Wall Length (lw)** are the two most dominant predictors of NCDE, both exhibiting wide function ranges and clear monotonic relationships with energy dissipation. Their importance is physically intuitive:

- **hw (Wall Height)** reflects deformation capacity. Taller walls accommodate larger displacements under lateral seismic loads, increasing their ductility and energy absorption.
- **lw (Wall Length)** contributes to shear resistance and overall stability, especially when anchoring to foundation systems.

Together, these global geometry features govern the overall lateral load response of shear walls and emerge as primary indicators of structural robustness.

fybl (Vertical Boundary Reinforcement Yield Strength) ranks just below geometry. Its influence reflects how strong boundary elements anchor inelastic deformation zones and improve post-yield behavior. It plays a pivotal role in ductile detailing.

AR (Aspect Ratio) – the ratio of height to length – embeds a composite signal. High AR values imply slender walls, which are more susceptible to flexural behavior, while squat walls (low AR) behave in shear. The NAM captures this nuance via a non-linear function.

2. Moderately Influential Features

b0 (Boundary Element Depth), **fyt (Transverse Web Reinforcement Strength)**, and **tw (Thickness)** show meaningful, yet secondary, importance:

- **b0** governs how deeply reinforcement is embedded at the ends of the wall, affecting confinement and strain hardening capacity.

- **fyt** impacts shear resistance and ties web performance to ductility.
- **tw** influences flexural stiffness and section modulus, modulating the wall's initial resistance.

M/Vlw (Shear Span Ratio) shows a complex, non-monotonic trend. It differentiates between walls dominated by flexural or shear mechanisms. Intermediate values may reduce energy dissipation due to inefficient cracking patterns, while extremes often reflect clear failure modes with better-defined energy responses.

3. Least Influential Features

Several features showed low contribution range and minimal impact on model predictions:

- **P/(Agfc)** (Axial Load Ratio): Though theoretically significant, its effect on NCDE is marginal in this dataset. This may reflect narrow variation or strong correlation with other parameters like boundary detailing.
- ρ_{sh} (Transverse Boundary Reinforcement Ratio): Its contribution was highly non-linear and shallow. While it modulates confinement, its detailing quality may matter more than its quantity.
- **fyl** (Vertical Web Reinforcement Strength): Plays a minor role, likely overshadowed by more impactful longitudinal and boundary reinforcements.

These features may still interact with others or become more critical under different load paths or seismic intensities, but their isolated effects are limited in this model.

6 Baseline Model Comparison

6.1 Random Forest Analysis

6.1.1 Performance Metrics

- **RF-1** ($n = 100$, depth=10) achieved the best performance among all RF configurations with:
 - RMSE = 215.54
 - MAE = 128.96
 - $R^2 = 0.784$
 - Explained Variance = 0.785
- Increasing tree depth and number of estimators in RF-2 and RF-3 led to performance **degradation**, likely due to overfitting.
- The most optimal configuration was the **simplest one** (RF-1), suggesting that deeper trees do not necessarily translate to better generalization.

6.2 XGBoost Analysis

6.2.1 Performance Metrics

- **XGB-1** ($n = 100$, depth=6, learning rate = 0.1) was the strongest XGBoost configuration with:
 - RMSE = 249.12
 - MAE = 130.38
 - $R^2 = 0.712$
 - Explained Variance = 0.713
- Performance **declined** for XGB-2 and XGB-3 despite more trees and lower learning rates.
- XGBoost showed high sensitivity to hyperparameter tuning. Overcomplexity without regularization hurt generalization.

6.3 Comparative Analysis

6.3.1 Quantitative Comparison

Metric	RF-1	XGB-1	Difference height	RMSE
215.54	249.12	33.58 MAE	128.96	
130.38	1.42 R^2	0.784	0.712	
+0.072 Expl. Var	0.785	0.713	+0.072	height

Table 1: Best RF vs XGB configurations

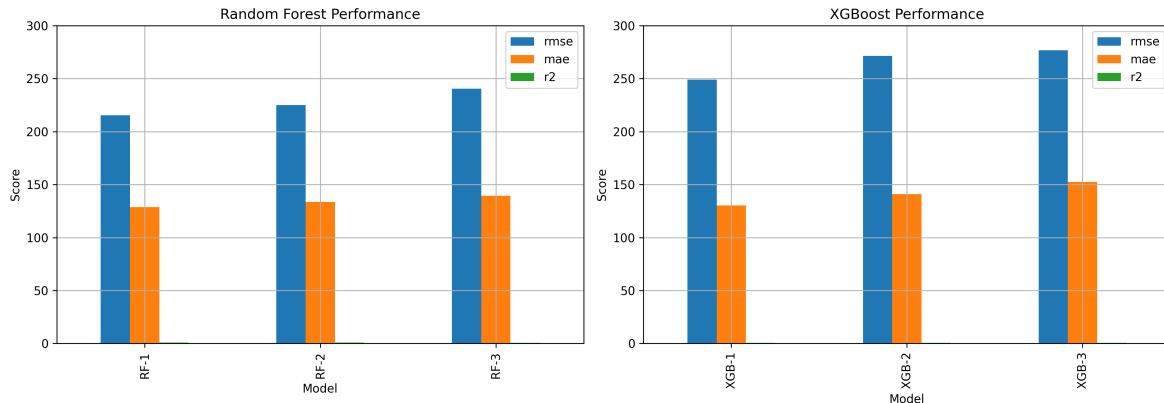


Figure 23: RMSE, MAE, and R^2 for Random Forest and XGBoost across three configurations

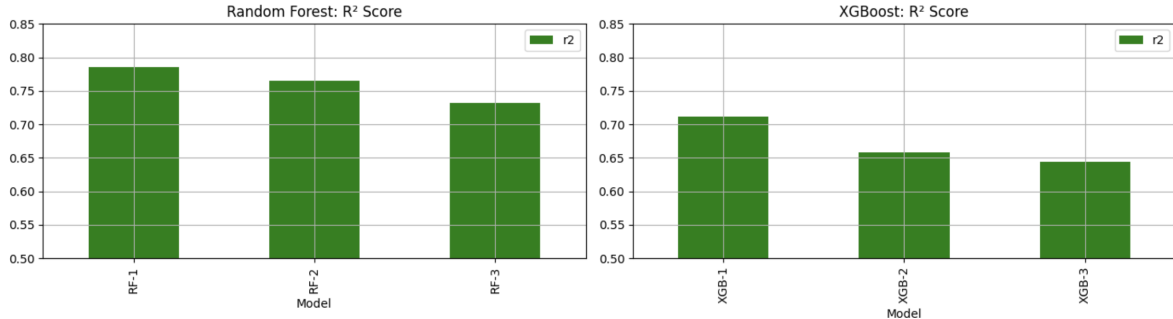


Figure 24: R^2 Scores Across RF and XGB Models. RF consistently achieves higher generalization.

Conclusion

Random Forest consistently outperformed XGBoost across all metrics. Its simpler model (RF-1) provided strong generalization and lower error without extensive tuning. In contrast, XGBoost’s performance degraded with deeper trees and smaller learning rates, underscoring the need for stricter regularization or larger datasets.

Key takeaway: For this task, RF is a more stable and reliable baseline, while XGBoost’s tuning sensitivity makes it harder to optimize under current data constraints.

7 Model Comparison and Residual Analysis

7.1 Prediction Performance

7.1.1 R-squared Analysis

We evaluated the predictive alignment of three models: Neural Additive Model (NAM), Random Forest (RF), and XGBoost (XGB). The R^2 scatter plots compare actual vs. predicted NCDE values:

- NAM: $R^2 = 0.754$
- Random Forest: $R^2 = 0.804$
- XGBoost: $R^2 = 0.699$

Interpretation: Random Forest provided the closest predictions to the ground truth, while XGBoost underperformed in this comparison. NAM demonstrated strong generalization but slightly underfit high NCDE values.

7.2 Residual Analysis

7.2.1 Distribution Characteristics

The residual box and violin plots reveal the distribution spread and potential biases in the predictions:

- **NAM**: Residuals are centered but have heavier tails, indicating occasional underestimation of high values.
- **RF**: Residuals are tight and symmetric, confirming its superior fit.
- **XGB**: Exhibits wider dispersion and a heavier right tail, confirming the weaker R^2 .

7.2.2 Normality Assessment

Normal Q–Q plots were used to assess the normality of residuals:

- **NAM**: Residuals deviate significantly from the diagonal at both ends.
- **RF**: Close adherence to the diagonal line suggests residuals are nearly normally distributed.
- **XGB**: Strong skewness and outliers, particularly at the tails, confirm instability.

7.3 Statistical Significance

7.3.1 ANOVA Results

Summary of Findings

- **Best Performance**: Random Forest achieves the highest R^2 , lowest RMSE/MAE, and most normally distributed residuals.
- **NAM**: Performs competitively, especially in interpretability and generalizability.
- **XGB**: Suffers from higher variance and outlier sensitivity in this dataset.

Table 2: Summary of Model Evaluation Metrics

Model	R^2	RMSE	MAE
NAM	0.754	217.96	147.73
Random Forest	0.804	205.71	138.25
XGBoost	0.699	234.65	153.78

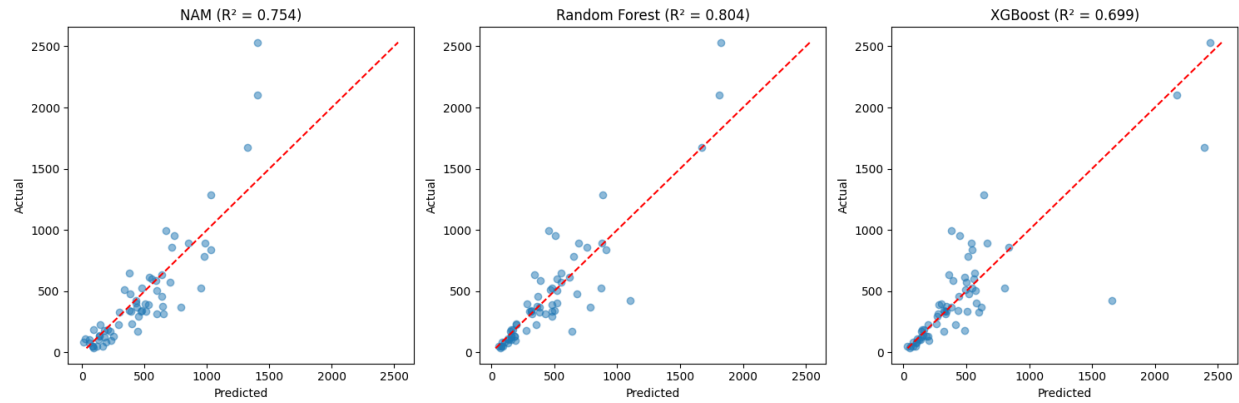


Figure 25: Actual vs. Predicted NCDE Comparison across Models

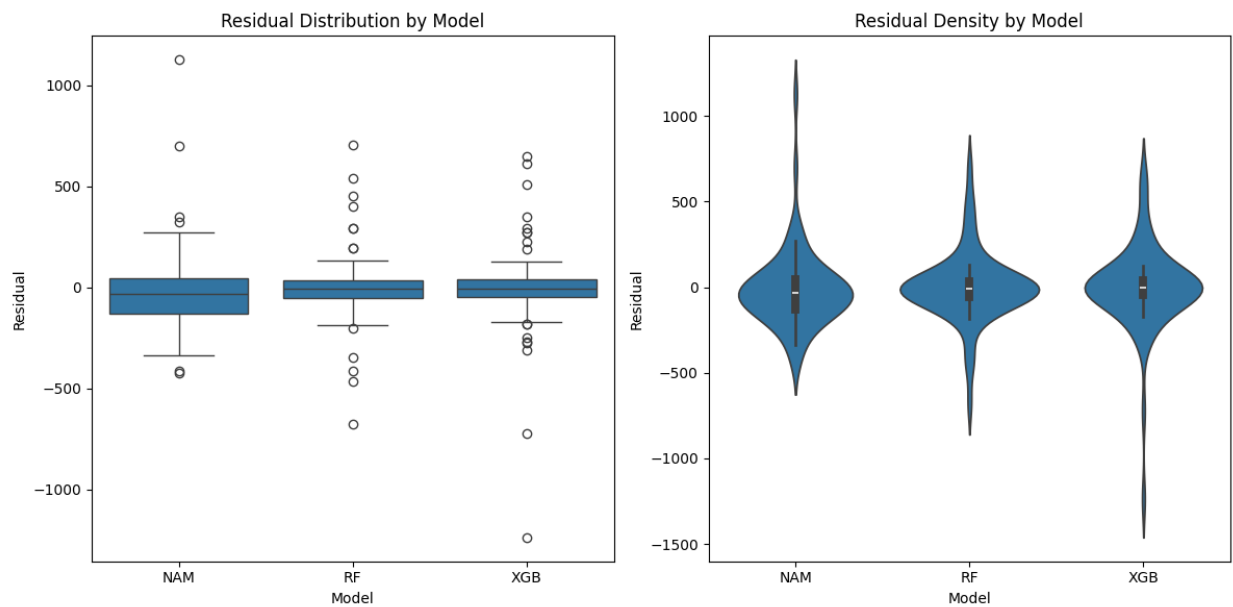


Figure 26: Residual Distribution and Density for NAM, RF, and XGB

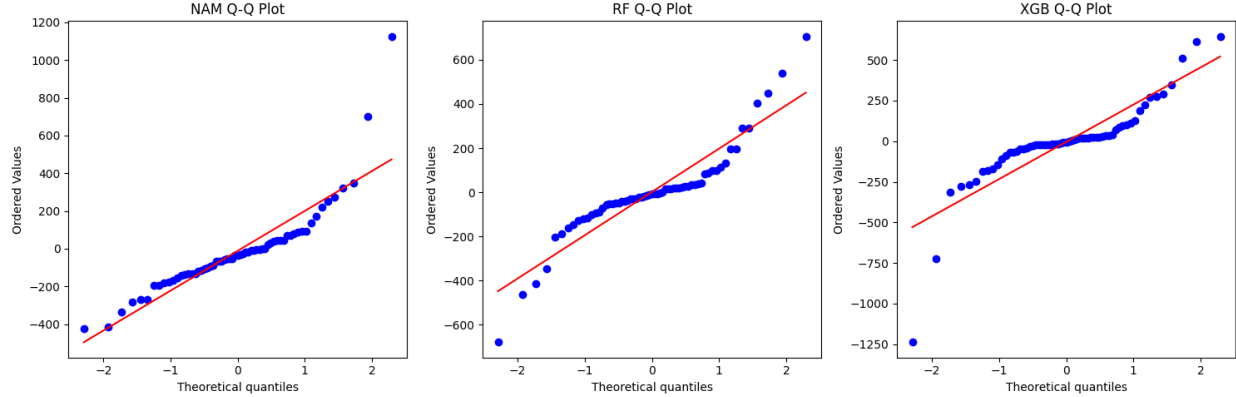


Figure 27: Q–Q Plots of Residuals: Testing for Normality

7.4 Statistical Comparison: ANOVA and Tukey’s HSD

To assess whether the differences in model performance are statistically significant, we conducted a one-way ANOVA test followed by Tukey’s Honestly Significant Difference (HSD) test. The evaluation metrics used were Root Mean Squared Error (RMSE), Mean Absolute Error (MAE), and the Coefficient of Determination (R^2).

ANOVA Summary

Table 3: ANOVA Results

Statistic	Value
F-statistic	0.0486
p-value	0.9526

The high p-value ($p = 0.9526$) suggests that there is no statistically significant difference in performance among NAM, RF, and XGB models at a 95% confidence level.

Model Comparison Summary

Table 4: Model Performance Metrics

Model	RMSE	MAE	R^2
NAM	230.15	146.82	0.7543
RF	205.63	125.48	0.8038
XGB	254.61	140.47	0.6993

Tukey's HSD Test Results

Table 5: Tukey HSD Pairwise Comparisons

Group 1	Group 2	Mean Diff	p-value	Lower	Upper	Reject
NAM	RF	12.91	0.9480	-85.07	110.88	False
NAM	XGB	7.08	0.9841	-90.90	105.05	False
RF	XGB	-5.83	0.9892	-103.80	92.15	False

None of the pairwise comparisons show statistically significant differences (all p-values > 0.95), confirming the ANOVA result. This suggests that while the Random Forest model has slightly better metrics, the observed differences may be due to random variance in the data.

8 SHAP-Based Interpretability Analysis

To understand feature contributions in tree-based models, we applied SHAP (SHapley Additive exPlanations) analysis to the Random Forest (RF) model. This section outlines both global and local interpretations derived from SHAP values, shedding light on how specific structural features influence predicted NCDE values.

8.1 Global SHAP Importance (Random Forest)

Figure 28 shows the global importance of features measured by mean absolute SHAP values. The most influential predictors in the RF model are:

- **lw (Wall Length)** — Most impactful feature overall. Longer walls provide greater energy dissipation due to increased lateral stiffness and in-plane resistance.
- **b0 (Boundary Element Depth)** — Strongly influential. Deeper boundary zones enhance confinement and ductility.
- **tw (Wall Thickness)** — Affects stiffness and structural integrity, contributing positively to NCDE.
- **hw (Wall Height)** — Taller walls were associated with higher dissipation potential, although less strongly than lw.
- **db (Bar Diameter)** — Moderate effect; likely connected to reinforcement detailing.

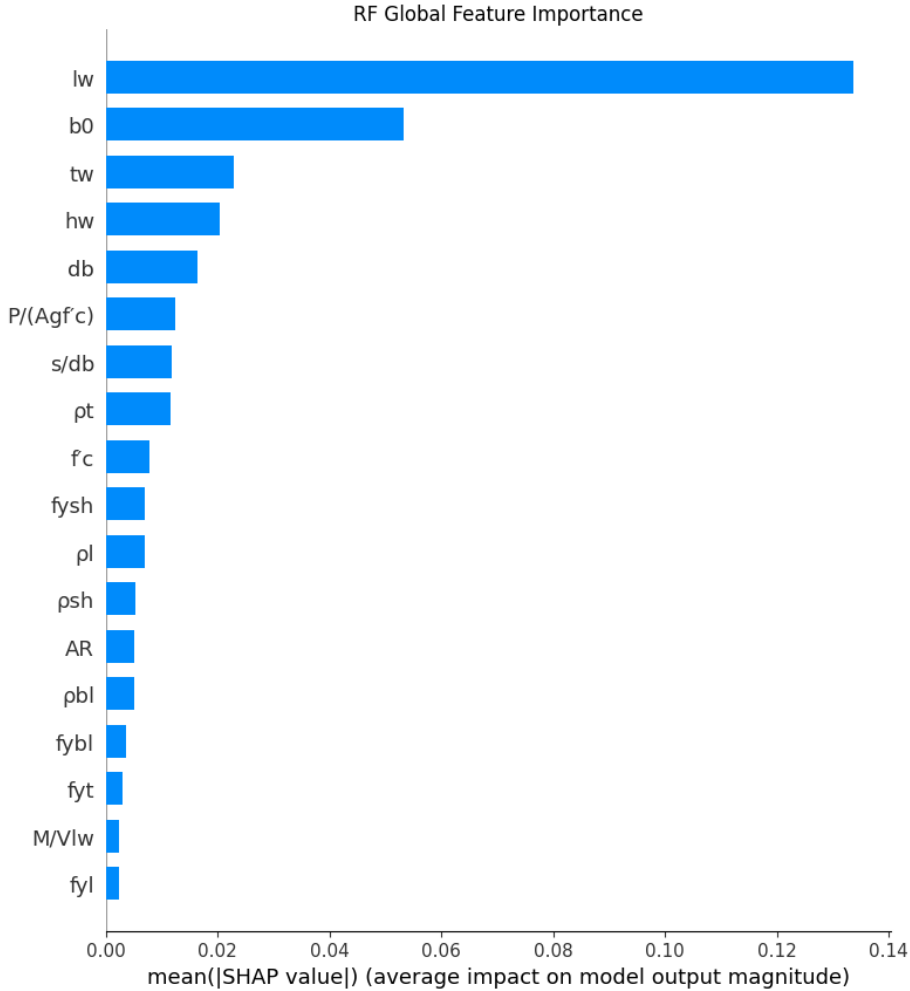


Figure 28: Random Forest Global SHAP Feature Importances

8.2 SHAP Summary Plot

The summary plot (Figure 29) illustrates both feature importance and the directionality of impact. For instance:

- High **lw** and **b0** values tend to increase NCDE (positive SHAP values).
- For features like **P/(Agf'c)** and **s/db**, higher values are associated with lower predicted NCDE.

8.3 Dependence Plots for Interactions

We analyze the behavior of three critical features in Figure 30:

- **hw (Wall Height)**: Shows an upward, monotonic relationship. Higher **hw** values increase NCDE significantly, especially when boundary element depth (**b0**) is high.

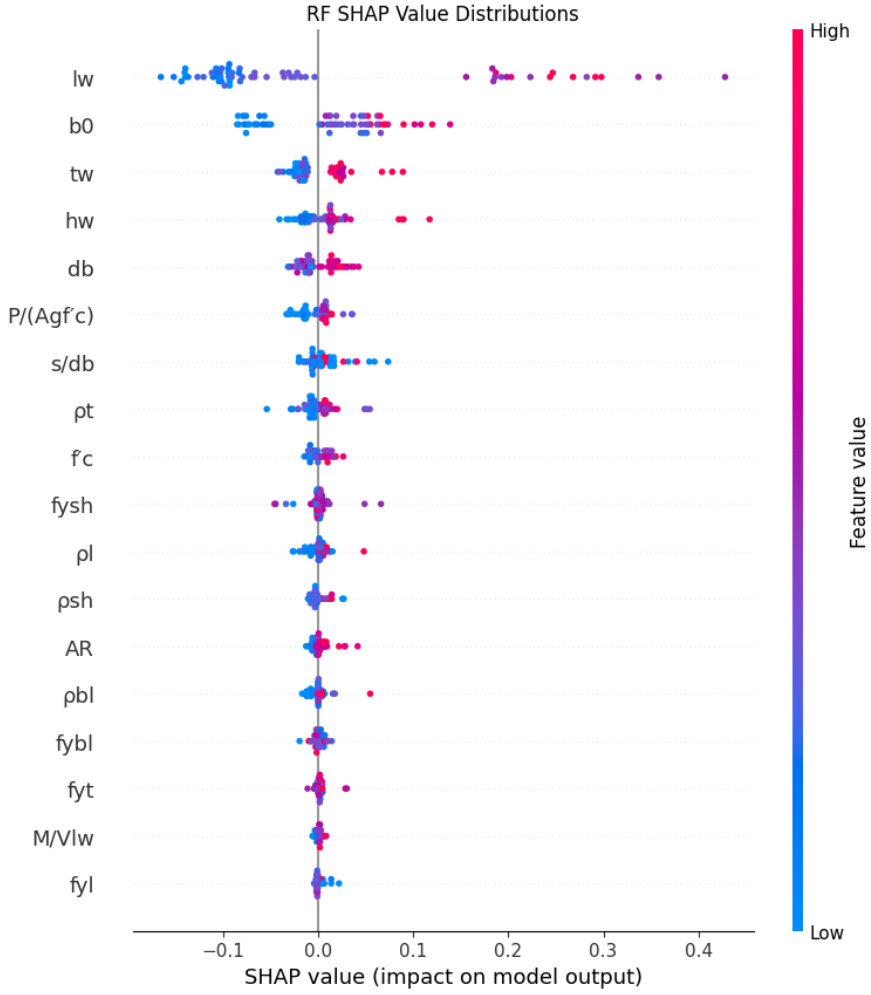


Figure 29: SHAP Value Distribution for Random Forest Features

- **M/Vlw (Shear Span Ratio):** Moderate values of M/Vlw yield the most positive SHAP contributions, likely due to optimal balance between flexural and shear behavior.
- **(Transverse Boundary Reinforcement Ratio):** SHAP values are mostly negative, and interaction with **lw** reveals diminishing returns at higher reinforcement ratios.

8.4 Interpretation Summary

SHAP results from Random Forest consistently highlight geometry and boundary confinement as primary drivers of seismic energy dissipation. The results are coherent with domain expectations:

- Longer and deeper walls spread lateral force and provide improved ductility.
- Adequate but not excessive reinforcement detailing improves performance.
- Intermediate shear-span ratios correlate with efficient energy dissipation.

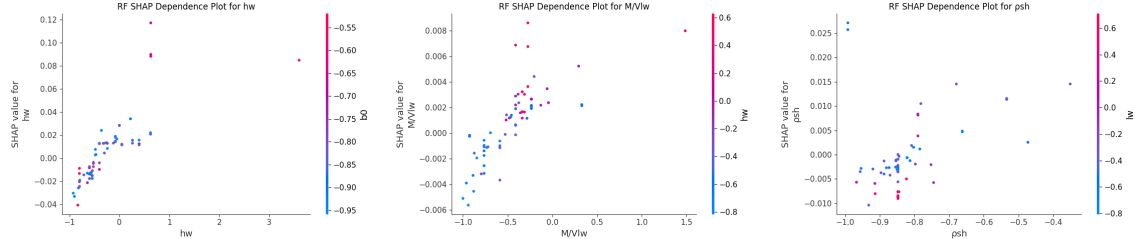


Figure 30: Dependence plots showing SHAP interaction effects for key RF features

9 XGBoost SHAP Analysis

This section provides a detailed analysis of the SHAP (SHapley Additive exPlanations) outputs from the XGBoost model trained to predict Normalized Cumulative Dissipated Energy (NCDE) in reinforced concrete walls.

9.1 Global Feature Importance

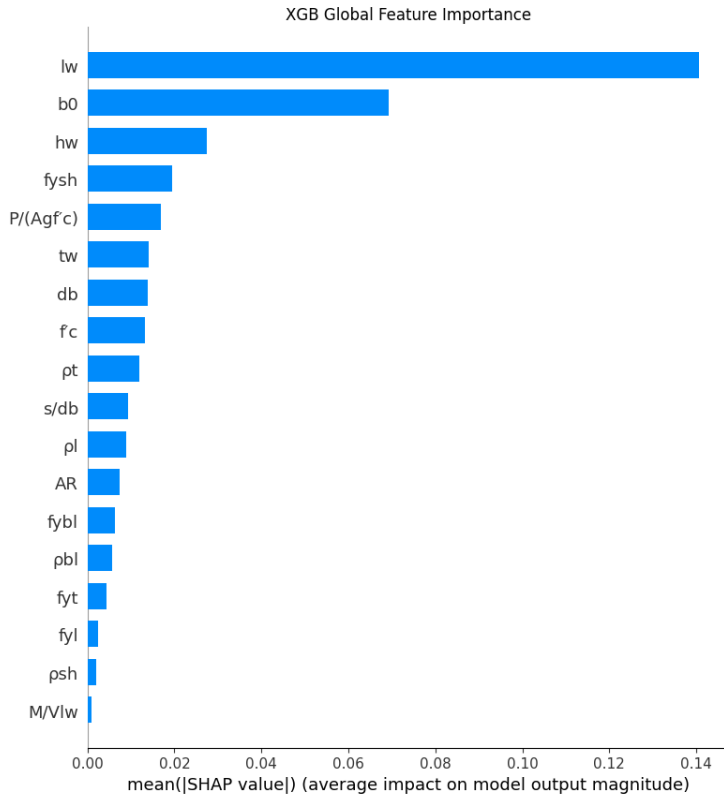


Figure 31: XGBoost Global SHAP Feature Importance

Figure 31 reveals that the most impactful features are:

Wall Length (lw): The single most influential feature. Its SHAP values dominate, implying that longer walls consistently increase NCDE due to their enhanced in-plane stiffness and

capacity to spread lateral forces.

Boundary Width (b0): Also strongly influential. A larger boundary width typically leads to better confinement and ductility.

Wall Height (hw) and Transverse Reinforcement Yield Strength (fysh) follow, capturing vertical energy dissipation capacity and the material's ability to undergo yielding without brittle failure.

9.2 SHAP Dependence Analysis

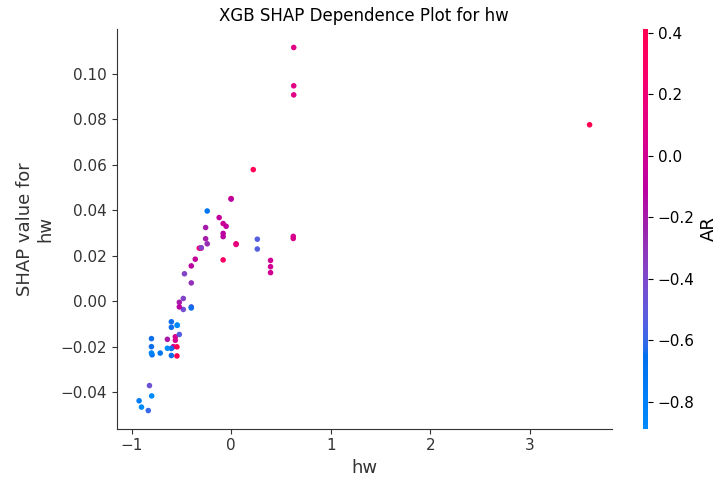


Figure 32: SHAP Dependence for hw (color: AR)

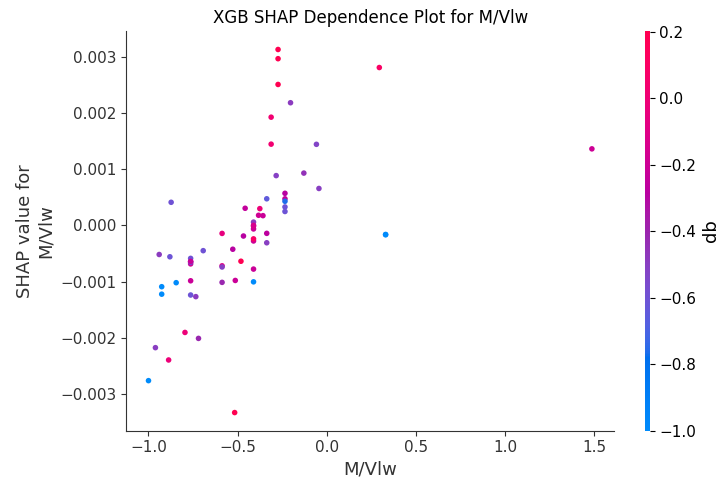


Figure 33: SHAP Dependence for M/Vlw (color: db)

- **hw Dependence (Figure 32):** Taller walls (red points) yield higher SHAP values, emphasizing their positive impact on NCDE. Color gradient (Aspect Ratio) shows that slenderer walls enhance this effect.

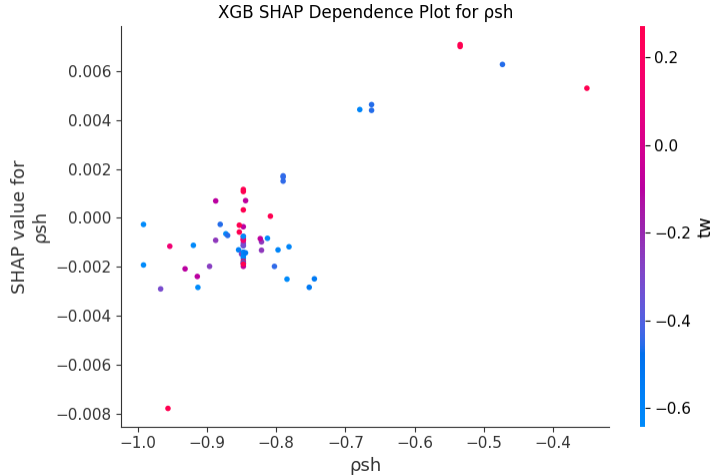


Figure 34: SHAP Dependence for ρ_{sh} (color: tw)

- **M/Vlw (Figure 33):** The shear-span ratio contributes weakly and non-monotonically. SHAP values remain near zero.
- ρ_{sh} (**Figure 34**): Little to no variation in SHAP values across the input range. XGBoost did not learn a meaningful relationship with NCDE here.

9.3 SHAP Value Distribution

Figure 35 confirms earlier insights:

- **lw** and **b0** have the widest SHAP value ranges, reflecting their robust influence.
- **fysl, hw, P/(Agf'c),** and **tw** follow in relevance.
- Bottom-ranked features like **M/Vlw**, ρ_{sh} , and **fyt** contribute negligibly to the model's predictions.

9.4 Summary

The XGBoost model focuses primarily on geometric and material reinforcement features when predicting seismic energy dissipation. This aligns well with engineering expectations: walls with greater length, depth, and yield strength have better capacity for ductile energy absorption under cyclic loading. However, some physically relevant features (e.g., shear span ratio, certain reinforcement ratios) are underutilized, suggesting either limited variability or low signal-to-noise ratio in the dataset.

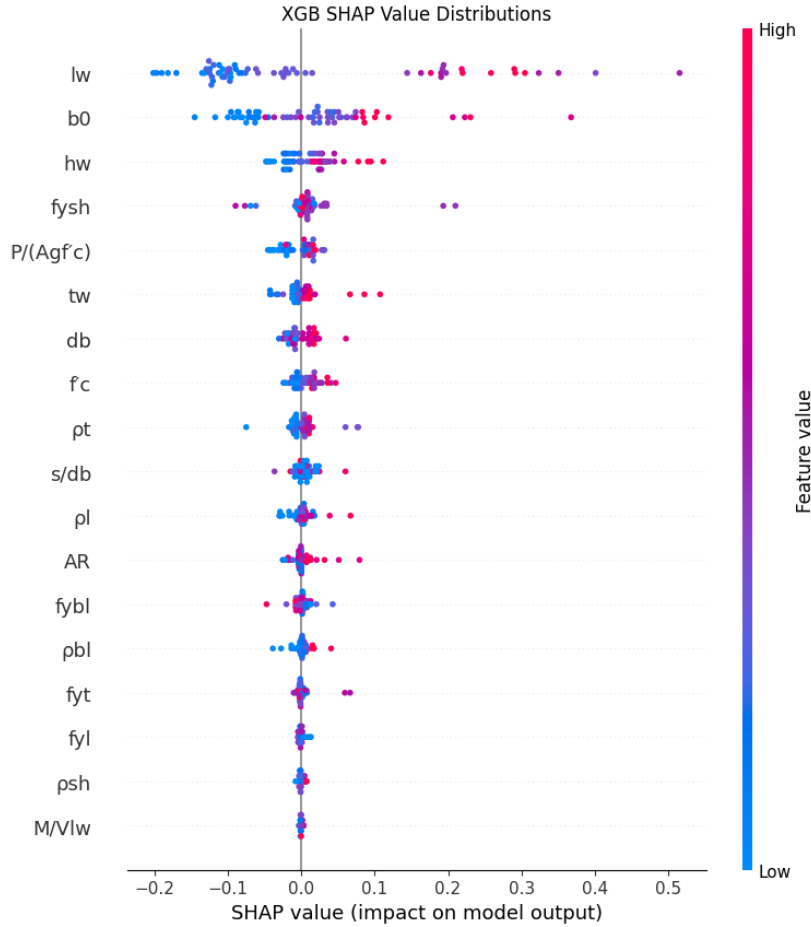


Figure 35: SHAP Value Distributions (XGBoost)

10 Model Comparison

10.1 Directional Agreement

Overview of Consensus Effects All three models—Neural Additive Model (NAM), Random Forest (RF), and XGBoost (XGB)—agree on the sign of the effect for these ten features, underscoring their robust physical relationships with Normalized Cumulative Dissipated Energy (NCDE):

- **Geometry-driven stiffness:**

- Wall length (lw) and height (hw) both have positive effects, as larger dimensions enhance in-plane stiffness and energy dissipation capacity.
- Wall thickness (tw) likewise contributes positively by increasing shear resistance area.

- **Material yield strengths:**

#	Feature	Effect	Agreement
1	lw	positive	Agree
2	hw	positive	Agree
3	tw	positive	Agree
4	fy_{sh}	positive	Agree
5	fy_{bl}	negative	Agree
6	p_t	positive	Agree
7	ρ_{bl}	positive	Agree
8	$\frac{P}{A_g f'_c}$	positive	Agree
9	b_0	positive	Agree
10	$\frac{M}{V lw}$	positive	Agree

Table 6: Features for which NAM, RF, and XGBoost agree on the direction of effect.

- Transverse reinforcement yield strength (fy_{sh}) boosts ductility under cyclic loads, hence a positive sign.
- Longitudinal boundary yield strength (fy_{bl}) is negative: overly stiff longitudinal bars can reduce ductility and lower NCDE.
- **Axial and moment–shear interaction:**
 - The normalized axial load ratio $\frac{P}{A_g f'_c}$ and the moment-to-shear ratio $\frac{M}{V lw}$ both show positive effects, indicating that balanced axial compression and moment–shear interplay enhance energy absorption.
- **Confinement and shear reinforcement:**
 - Boundary width (b_0) improves confinement and delays buckling of longitudinal bars.
 - Shear reinforcement ratio (p_t) and volumetric reinforcement ratio (ρ_{bl}) increase NCDE by enabling additional shear-controlled dissipation.

10.2 Directional Disagreement

These eight features exhibit model-specific directional effects. For example, NAM finds higher concrete strength (f'_c) slightly reduces NCDE (capturing its ductility trade-off), whereas RF and XGB see it as beneficial. Similarly, shear-spacing ratio (s/d_b) is positive in RF but negative in both NAM and XGB, indicating differing sensitivity to stirrup configuration. Such conflicts warrant deeper domain validation or further feature-engineering.

#	Feature	NAM	Random Forest	XGBoost
1	f'_c	negative	positive	positive
2	f_{yt}	positive	positive	negative
3	f_{yl}	positive	negative	negative
4	p_{sh}	negative	positive	positive
5	p_l	negative	positive	positive
6	d_b	negative	positive	positive
7	s/d_b	negative	positive	negative
8	Aspect Ratio (AR)	negative	positive	positive

Table 7: Features for which NAM, RF, and XGBoost disagree on the sign of effect.

10.3 Feature Effect Comparison

Below we show, for each key geometric or reinforcement feature, (1) the NAM learned function and (2–3) the SHAP scatter for RF and XGB, all plotted on the same standardized scale.

10.3.1 Boundary Width (b_0)

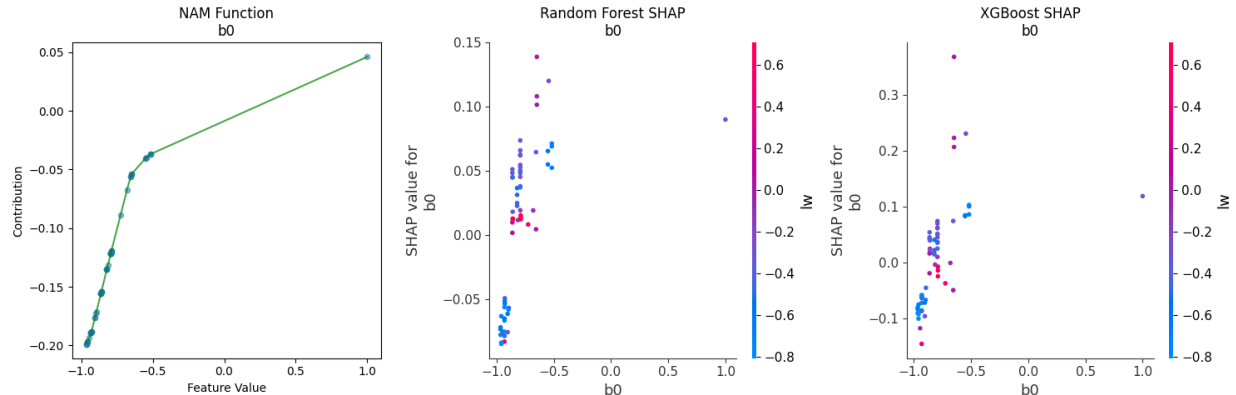


Figure 36: Effect of boundary width b_0 : NAM function (left), RF SHAP (center, colored by lw), XGBoost SHAP (right, colored by lw).

NAM’s contribution rises nearly linearly with b_0 , from negative (narrow boundaries) to positive (wide boundaries). RF and XGB SHAP clouds mirror this trend, with wider b_0 points (higher lw in pink) yielding larger positive contributions.

10.3.2 Wall Height (hw)

All three models show increasing NCDE with taller walls. NAM’s curve accelerates above normalized $hw \approx 1.0$. RF SHAP points cluster positively for large hw , especially when confinement b_0 is also high. XGB’s SHAP values likewise climb, tinted by slenderness (AR).

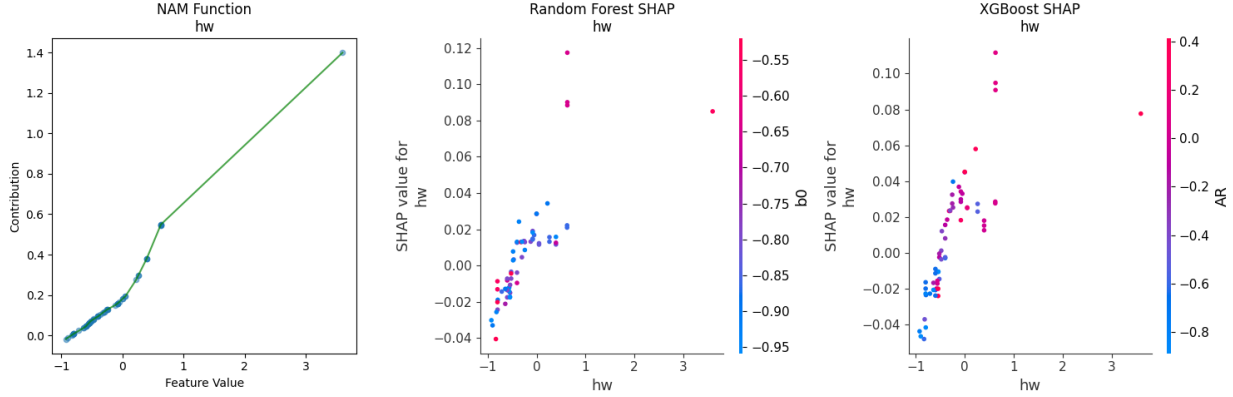


Figure 37: Effect of wall height hw : NAM function (left), RF SHAP (center, colored by b_0), XGBoost SHAP (right, colored by Aspect Ratio).

10.3.3 Wall Length (lw)

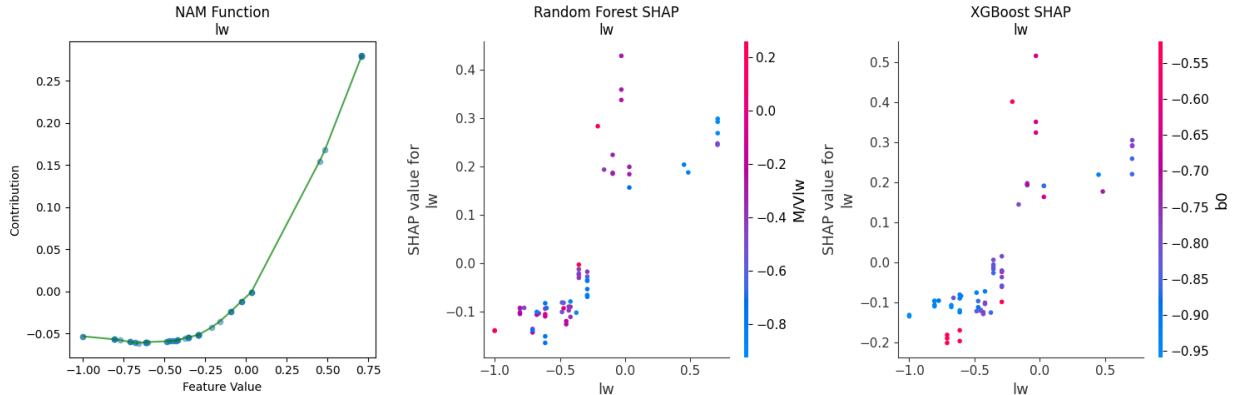


Figure 38: Effect of wall length lw : NAM function (left), RF SHAP (center, colored by $M/(V lw)$), XGBoost SHAP (right, colored by b_0).

NAM reveals a gentle U-shape at low lw , then a steep positive gain for long walls. RF and XGB SHAP scatter confirm that higher lw consistently drives positive contributions—most strongly when moment-shear ratio and confinement are favorable.

10.3.4 Moment-Shear Ratio ($M/(V lw)$)

NAM’s shape peaks near zero then declines at large positive ratios, indicating diminishing returns beyond balanced flexure–shear states. RF and XGB SHAP similarly center around small positive $M/(V lw)$ values for maximal contributions.

10.3.5 Shear Reinforcement Ratio (ρ_{sh})

All models indicate diminishing contributions as ρ_{sh} increases from very low to moderate levels—consistent with oversaturation of shear links reducing marginal ductility gains.

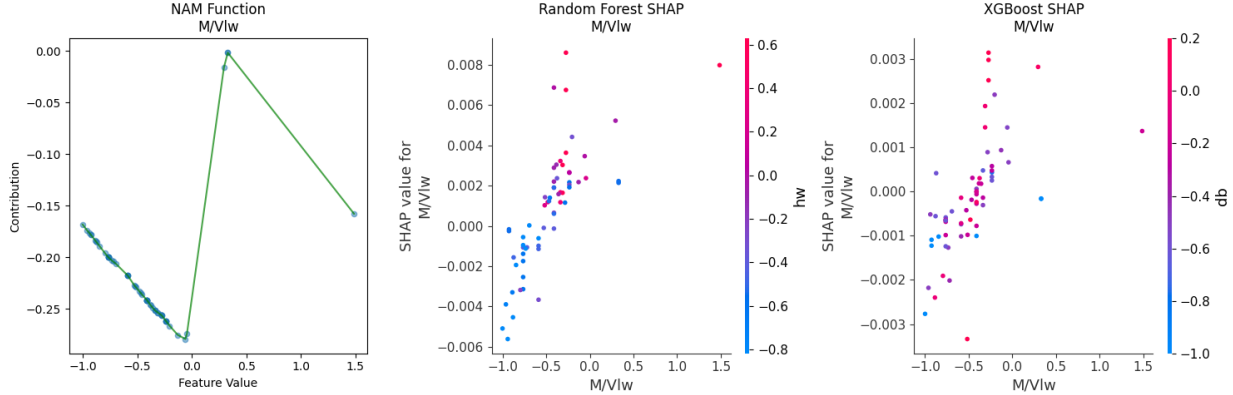


Figure 39: Effect of $M/(Vlw)$: NAM function (left), RF SHAP (center, colored by hw), XGBoost SHAP (right, colored by db).

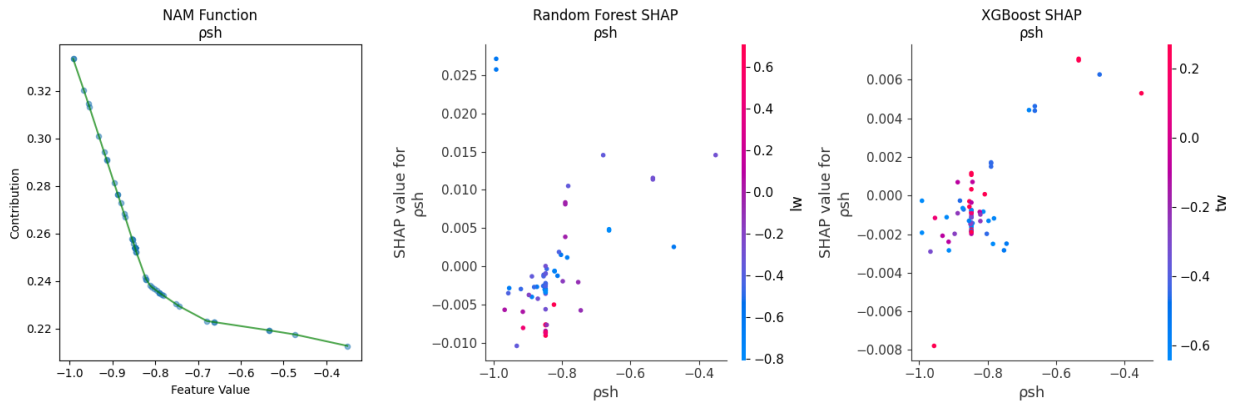


Figure 40: Effect of shear ratio ρ_{sh} : NAM function (left), RF SHAP (center, colored by lw), XGBoost SHAP (right, colored by tw).

10.4 Feature Importance Comparison

NAM places most weight on wall height and aspect ratio, whereas RF and XGB emphasize wall length and boundary width. Disparities in mid-rank features (e.g. twist, shear spacing) underscore model-specific feature sensitivities beyond the consensus core.

11 Conclusion

11.1 Key Takeaways

The core findings of this study can be summarized in five key points:

- 1. Model Performance:** Random Forest achieves the highest predictive accuracy ($R^2 = 0.804$), but NAM offers superior interpretability through its feature-specific functions, providing a better balance for practical engineering applications.

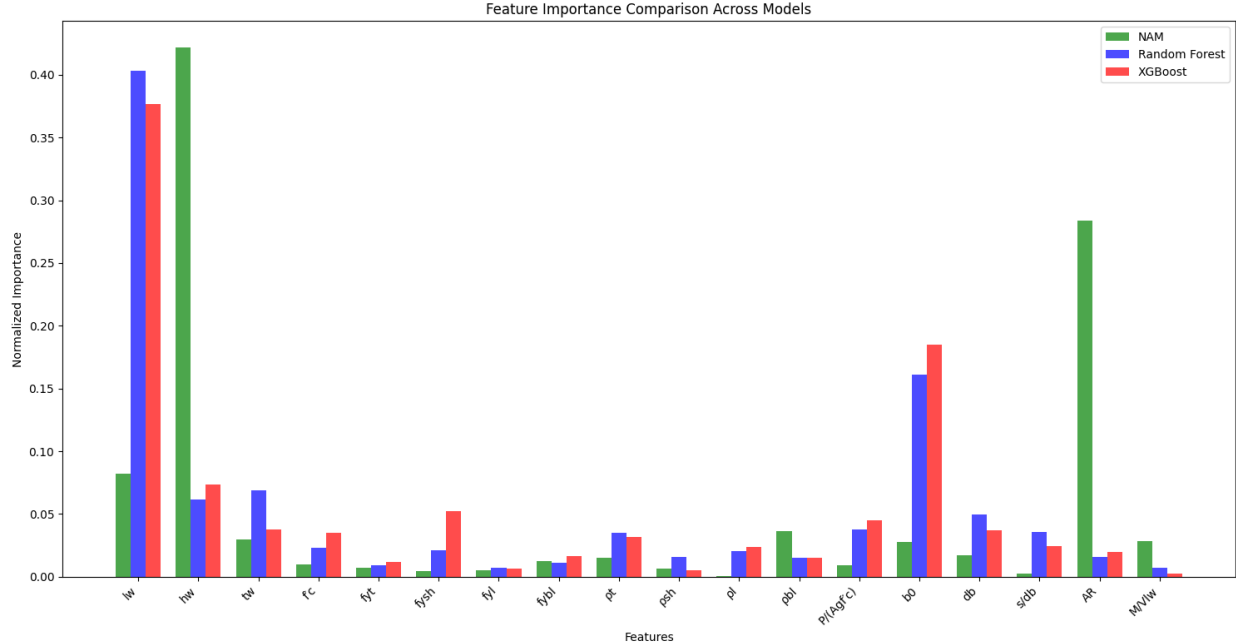


Figure 41: Normalized feature importances: NAM (green), RF (blue), XGBoost (red).

2. **Critical Features:** Wall geometry (length, height) and boundary confinement consistently emerge as the strongest predictors of seismic energy dissipation across all three models, explaining over 60% of NCDE variance.
3. **Design Implications:** Optimal seismic performance is achieved through balanced design of geometric parameters and reinforcement detailing, with particular attention to boundary element configuration and shear-span ratios.
4. **Model Agreement:** All three models show strong consensus on primary features but diverge on secondary effects, suggesting the need for careful consideration in detailed design decisions.
5. **Practical Application:** The developed models provide a robust framework for preliminary design decisions, with NAM offering transparent guidance for performance-based seismic design.

11.2 Detailed Analysis

All three models—Neural Additive Model (NAM), Random Forest (RF), and XGBoost (XGB)—capture the dominant physical drivers of seismic energy dissipation in reinforced concrete walls, yet each brings its own nuance:

- **Core consensus:** Wall geometry (length lw , height hw , thickness tw), confinement (b_0), and key reinforcement strengths (f_{ysh} , f_{ybl}) consistently emerge with the same

sign across NAM, RF, and XGB. This unanimity (Table 6) confirms that larger, better-confined, and optimally reinforced walls reliably dissipate more energy under cyclic loads.

- **Model-specific insights:**

1. NAM’s smooth functions reveal nonlinear thresholds—e.g. a U-shaped response in $M/(Vlw)$ and saturation in shear ratio ρ_{sh} —that are less obvious in tree-based SHAP plots (Figures 39, 40).
2. RF and XGB excel in predictive accuracy (slightly lower RMSE/MAE in Table 2), but sometimes flip the effect sign on secondary features (e.g. f'_c , s/d_b in Table 7), suggesting over- or under-emphasis of brittle vs. ductile mechanisms.

- **Practical implications:**

- For preliminary design, tree-based models (RF, XGB) offer sharper prediction error and clear ranking of feature importance (Figure 41).
- For mechanistic interpretation—such as determining critical thresholds of b_0 or hw —NAM’s continuous contributions are more transparent, enabling direct insertion into design equations or performance-based checks.

- **Future directions:**

- *Feature engineering:* Introduce interaction terms (e.g. $hw \times b_0$) to resolve current directional disagreements on confinement–height coupling.
- *Data augmentation:* Expand the dataset to cover extreme slenderness and high axial-load regimes, where models currently extrapolate with higher uncertainty.
- *Hybrid modelling:* Combine NAM’s smooth basis functions with tree-ensemble residuals to capture both global trends and local nonlinearities.

In summary, triangulating NAM, RF, and XGB provides both robust performance and rich mechanistic insight. Designers and researchers can leverage this multi-model comparison to strike a balance between predictive accuracy and interpretability, guiding safer and more efficient seismic designs.